I-29299   UK#0118-X

Y-12

Y-2359

OAK RIDGE
Y-12
PLANT

MARTIN MARIETTA

CHARACTERIZATION OF URANIUM SURFACES
MACHINED WITH AQUEOUS PROPYLENE
GLYCOL-BORAX OR PERCHLOROETHYLENE-
MINERAL OIL COOLANTS

S. S. Cristy
R. K. Bennett, Jr.
J. J. Dillon
H. L. Richards
R. D. Seals
V. R. Byrd

December 1986

DISCLAIMER

This report was prepared as an account of work sponsored by an agency of the United States Government. Neither the United States Government nor any agency Thereof, nor any of their employees, makes any warranty, express or implied, or assumes any legal liability or responsibility for the accuracy, completeness, or usefulness of any information, apparatus, product, or process disclosed, or represents that its use would not infringe privately owned rights. Reference herein to any specific commercial product, process, or service by trade name, trademark, manufacturer, or otherwise does not necessarily constitute or imply its endorsement, recommendation, or favoring by the United States Government or any agency thereof. The views and opinions of authors expressed herein do not necessarily state or reflect those of the United States Government or any agency thereof.

Date of Issue: December 31, 1986
Distribution Category: UC-25

Y--2359

DE87 004569

CHARACTERIZATION OF URANIUM SURFACES MACHINED WITH AQUEOUS PROPYLENE GLYCOL–BORAX OR PERCHLOROETHYLENE–MINERAL OIL COOLANTS

S. S. Cristy
R. K. Bennett, Jr.
J. J. Dillon
H. L. Richards
R. D. Seals
V. R. Byrd

DISCLAIMER

MASTER

DISTRIBUTION OF THIS DOCUMENT IS UNLIMITED

ABSTRACT

The use of perchloroethylene (perc) as an ingredient in coolants for machining enriched uranium at the Oak Ridge Y-12 Plant has been discontinued because of environmental concerns. A new coolant was substituted in December 1985, which consists of an aqueous solution of propylene glycol with borax (sodium tetraborate) added as a nuclear poison and with a nitrite added as a corrosion inhibitor.

Uranium surfaces machined using the two coolants were compared with respect to residual contamination, corrosion or corrosion potential, and surface morphology. Corrosion resistance of enriched uranium machined with the aqueous propylene glycol-borax coolant was found to be better than that of enriched uranium machined with the perc-mineral oil coolant. The boron residues on the final-finished parts machined with the borax-containing coolant were not sufficient to cause problems in further processing. All evidence indicates that the enriched uranium surfaces machined with the borax-containing coolant will be as satisfactory as those machined with the perc coolant.

3

CONTENTS

4

SUMMARY

Because of environmental concerns, perchloroethylene (perc) was eliminated as an ingredient in coolants used for machining enriched uranium at the Oak Ridge Y-12 Plant. A substitute coolant consisting primarily of an aqueous solution of propylene glycol and borax was formulated. The changeover to the new coolant occurred in December 1985. Thus, it is imperative to characterize uranium surfaces that have been machined with this new coolant and to compare them with those machined with the formerly used coolant with respect to residual contamination, corrosion or corrosion potential, and surface morphology to ensure that product quality and fitness for use are not endangered.

Enriched uranium machined with the aqueous propylene glycol-borax coolant was found to be more corrosion resistant than enriched uranium machined with the perc-mineral oil coolant. The boron residues on the final-finished parts machined with the borax-containing coolant are not sufficient to cause problems in further processing. All evidence indicates that the enriched uranium surfaces machined with the borax-containing coolant will be as satisfactory as those machined with the perc coolant.

INTRODUCTION

The use of perchloroethylene (perc) as an ingredient in coolants for machining enriched uranium at the Oak Ridge Y-12 Plant was discontinued in December 1985 because of environmental concerns. A substitute coolant has been formulated and implemented. This coolant consists of an aqueous solution of propylene glycol (50-50 by volume) with 90 g/L of borax (sodium tetraborate) added as a nuclear poison, 1000 mg/L of a nitrite added as a corrosion inhibitor, and 10 mg/L of azure blue dye added as a visual identifier. Thus, it is imperative to characterize uranium that has been machined with this new coolant and to compare it with uranium machined with the old coolant with respect to residual contamination, corrosion or corrosion potential, and surface morphology to ensure that product quality and fitness for use are not compromised by the coolant change. Of particular interest are the contamination and oxidation of surfaces that receive additional processing at the Rocky Flats Plant.

CHARACTERIZATION OF URANIUM SURFACES

PRESENTATION OF EXPERIMENTAL WORK

The experimental work encompassed five major divisions: (1) surface contamination, with the major emphasis on the determination of boron residues; (2) characterization of the oxide and amount of oxide formation under normal conditions after machining; (3) characterization of the surface morphology and local corrosion of the machined uranium; (4) accelerated corrosion testing; and (5) coolant characterization. For each of these divisions, parts were machined in a normal manner with production and inspection resident times consistent with historic production experience. Parts machined with the perc coolant were compared with parts machined with the new boron-containing coolant.

Five of the test parts were packaged and sent to the Rocky Flats Plant for evaluation following certification. These five parts were exceptions in that the time spent at Warehouse 5 was reduced to 2 d. A sixth part to simulate these was cut into samples and coupons at the shipment date. Two each of the test and production parts were unpacked and cut into samples after following the schedule shown in Table 1. Four production parts and three test parts were unpacked, cleaned with 1,1,1-trichloroethane (used at Rocky Flats for cleaning these parts before storage), repacked in plastic bags from Rocky Flats, and stored on the high-rise storage racks in Building 9215 at Y-12. Two each of these were randomly selected and cut into samples after 1 month of storage. The remaining three parts will be stored for 6 months before being cut into samples.

Table 1. Average resident times for M-Wing part.

Location	Average resident time (d)
H-2 inspection	3
9212 radio	4
M-Wing dispatching (certify availability)	3
Quality liaison (certify)	4
M-Wing dispatching (cleaning and packing)	14
Warehouse 5	17
Total time after M-Wing final-finish machining	45
Range of total time after final-finish machining	29-55
Shipping to Rocky Flats	3
Time before unpacking	1

Table 2 is a summary of the parts and treatment history.

Table 2. Summary of parts and treatment history

Part	Treatment	Coolant
5715	Same as Rocky Flats test parts (standard[a] minus 15 days in Warehouse 5)	Boron[b]
5692 and 5713	Standard	Boron
5725 and 5726	Standard	Perc[c]
5720 and 5722	Standard plus 1-month storage in Rocky Flats bags	Boron
5730 and 5733	Standard plus 1-month storage in Rocky Flats bags	Perc
5727	Standard plus 6-month storage in Rocky Flats bags	Boron
5739 and 5740	Standard plus 6-month storage in Rocky Flats bags	Perc

Note: Parts 5597, 5700, 5701, 5717, and 5721 were shipped to the Rocky Flats Plant.

[a]Resident times as given in Table 1 (total handling plus storage time of 45 d).
[b]Aqueous solution of borax and propylene glycol.
[c]Perc—mineral oil.

SURFACE CONTAMINATION

Boron

A prime reason for this study was to determine if the new coolant left detrimental residues or residues that might be construed as detrimental, particularly boron, on the surfaces of the completed parts. Thus machine turnings or chips from the first 0.005 in. of the surface were collected from the mouth, 45°, and pole areas on both the inner contour (IC) and outer contour (OC) of the parts (Fig. 1). Enough chips were collected to make at least 6 g, and the surface area sampled was measured. These chips were then sent to the Y-12 Plant Laboratory for dissolution and boron analysis by inductively coupled plasma emission spectroscopy (ICP).

Bulk boron concentrations in the enriched uranium were obtained from chips or turnings from the debrimming or the face and step procedure; these concentrations were used as baseline data for the determination of surface boron by ICP analysis. The debrimming procedure is performed before semifinish machining and was done using the perc coolant. Table 3 shows these data.

Y-DWG 85-1196

COUPONS TO BE CUT FROM EACH PART

Fig. 1. Coupons to be cut from each part.
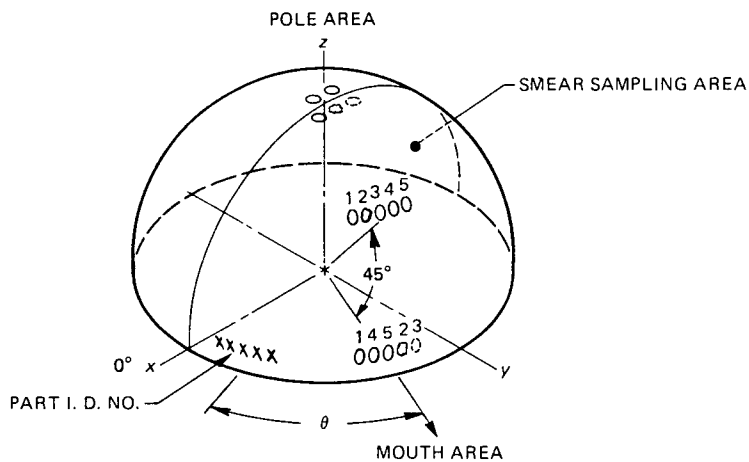
SAMPLE 1. ONE 0.7-in. DISK FROM EACH OF THE THREE LOCATIONS FOR IMMA AND SEM ANALYSIS

SAMPLE 2. CHIPS OR TURNINGS (5 g) CUT FROM THE FIRST 0.005 in. OF THE OC SURFACE AT EACH OF THE THREE LOCATIONS FOR ICP-SPECTROSCOPIC ANALYSIS

SAMPLE 3. CHIPS OR TURNINGS (5 g) CUT FROM THE FIRST 0.005 in. OF THE IC SURFACE AT EACH OF THE THREE LOCATIONS FOR ICP-SPECTROSCOPIC ANALYSIS

SAMPLE 4. ONE 0.75-in. DISK FROM EACH OF THE THREE LOCATIONS FOR ESCA ANALYSIS

SAMPLE 5. ONE 1.3-in. DISK FROM EACH OF THE THREE LOCATIONS FOR ACT ANALYSIS

SAMPLE 6. 2.4-in. DISKS, CUT AS SELECTED BY S. S. CRISTY

Table 3. Bulk ICP data from debrimming operation
(Values are parts per million by weight.)

Part	B	C	Cr	Al	Mn	Cu	Mo	Fe	Si	Ni
5725	0.36	375	10	20	10	10	50	100	175	30
5726	0.29	379	20	20	10	10	50	100	200	20
5730	0.25	420	20	20	10	10	60	100	200	22
5733	0.41	396	20	30	10	10	50	100	200	30
5739	0.44	377	20	20	15	10	60	100	200	40
5740	0.42	383	20	20	15	15	50	100	175	40
Average	0.36 ±0.08	388	13	22	13	11	53	100	192	30

The boron measurements from a second set of data varied more widely than those of this set and were not considered reliable. The boron in the substrate or bulk uranium may not be very homogeneously distributed,

thus leading to erroneous corrections when reducing the ICP data to determine surface boron from chips. The value of 0.36 ppm of boron in the uranium substrate was used to calculate the surface boron by difference.

Table 4 summarizes the amounts of surface contaminant boron as determined using chip data from the boron coolant-machined parts. The statistical F test applied to these data indicated that the quantity of IC surface boron was significantly greater than the quantity of OC surface boron. This same test indicated that the differences observed between pole, 45°, and mouth positions were also significant. On the IC, boron increased in the order of pole, 45°, mouth, whereas on the OC, the order was reversed (Fig. 2).
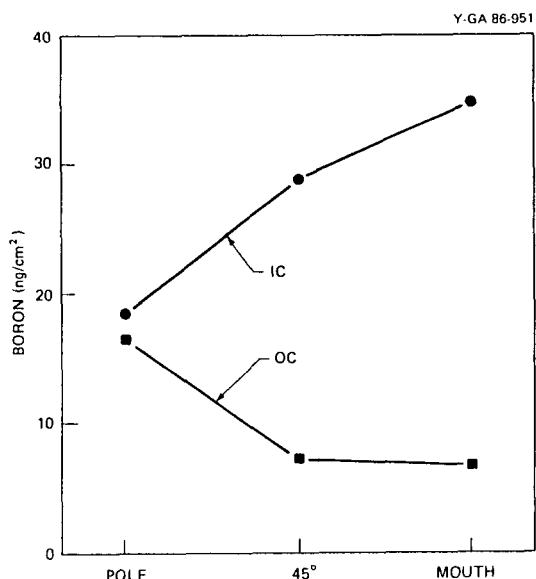

Fig. 2. Surface boron from chip data as a function of location.

Chip data were collected from only one of the perc-cut parts—part 5725, which had the standard handling treatment. The chips from the six locations on this part averaged 0.29 ± 0.05 ppm, less than the 0.36 ppm found for the bulk uranium (Table 3). Thus, the surface boron can only be said to be below our limits of certification.

As can be seen from Table 4, determination of boron by chip dissolution and ICP analysis yields data that vary greatly. The probable cause is a significant but inhomogeneously distributed quantity of boron in the base uranium. To circumvent this inhomogeneity and obtain an independent measure of the surface boron, two 6-cm-diam disks were cut from each part and acid leached to remove a thin layer of the surface and thus the boron residues. Boron and uranium in the leachant were

Table 4. Chip data determination of boron residues
on part surfaces from boron coolant-machined parts

Part	Treatment		Boron (ng/cm^2)	Surface
5715	Same as Rocky Flats		8.4	IC pole
	test parts		43	IC 45°
			36	IC mouth
		Average	29	IC
5715	Same as Rocky Flats		27	OC pole
	test parts		6.3	OC 45°
			0	OC mouth
		Average	11	OC
5715		Average	20	OC + IC
5692	Standard		24	IC pole
			42	IC 45°
			34	IC mouth
		Average	33	IC
5692	Standard		7.7	OC pole
			20	OC 45°
			18	OC mouth
		Average	15	OC
5692		Average	24	OC + IC
5713	Standard		36	IC pole
			31	IC 45°
			46	IC mouth
		Average	38	IC
5713	Standard		45	OC pole
			10	OC 45°
			14	OC mouth
		Average	23	OC
5713		Average	30	OC + IC
5720	Standard plus		24	IC pole
	1-month storage in		28	IC 45°
	Rocky Flats bags		57	IC mouth
		Average	36	IC
5720	Standard plus		3.5	OC pole
	1-month storage in		0	OC 45°
	Rocky Flats bags		2.8	OC mouth
		Average	2.8	OC
5720		Average	19	IC + OC
5722	Standard plus		0	IC pole
	1-month storage in		0	IC 45°
	Rocky Flats bags		1.1	IC mouth
		Average	0.4	IC
5722	Standard plus		0	OC pole
	1-month storage in		0	OC 45°
	Rocky Flats bags		0	OC mouth
		Average	0	OC
5722		Average	0.2	OC + IC
Grand averages and standard deviation			27 ± 15	IC
			10 ± 9	OC
			19 ± 15	IC + OC

determined by ICP spectrographic analysis. This method of sample preparation does not remove enough substrate or bulk uranium for the boron from this source to be analytically significant. A minor drawback is that ICs and OCs are not separated by this method. In Table 5, the results are compared with the sums of the IC and OC boron as determined from the chip data.

Table 5. Average boron residues for part surfaces
(IC + OC) determined from surface chips and
from acid leachings

| Part | Boron (ng/cm^2) | | Coolant |
	Acid leaching	Surface chips	
5715	12	20	Boron
5692	19	24	Boron
5713	16	30	Boron
5720	16	19	Boron
5722	13	0.2	Boron
5727	16	ND[a]	Boron
5725	ND	LDL[b]	Perc
5726	<7	ND	Perc
5730	<3	ND	Perc
5733	<3	ND	Perc
5739	<3	ND	Perc
5740	<3	ND	Perc
Average	15 ± 3	19 ± 15	Boron
Average	LDL	LDL	Perc

[a]Not determined.
[b]Less than detection limit.

Since a nondestructive technique for determining boron residues on surfaces would be desirable, a smear sampling method was tried. A 47-mm-diam cellulose acetate Millipore filter was found to be tough enough to withstand vigorous hand scrubbing of a part surface and was chosen for use over a Whatman filter, which crumbled with the same treatment. The filter was wet with triply distilled water, and an area of ~123 cm^2 was scrubbed with three filters. Approximately 20 mL of this water was used to rinse the scrubbed area and was collected with the filter papers. The filter papers were then digested, and the boron in the solutions was measured by ICP.

It was also of interest to determine whether boron residues on semifinish surfaces were comparable to those on final finishes and whether OCs were comparable to ICs. The boron on the semifinish ICs of 11 boron coolant-machined parts averaged 52 mg/cm^2 with a standard deviation of ±57 ng/cm^2. On the perc machined parts, boron averaged <8 ng/cm^2. On the final-finish surfaces, which included OC smears on

the five Rocky Flats parts and IC and OC smears on the other six boron coolant-machined parts and on the six perc coolant-machined parts, all boron determinations were below the detection limit of ~8 ng/cm^2.

To determine the effectiveness of the smearing technique for final-finish determinations, a 6-cm-diam coupon was cut from each of two smeared and two nonsmeared areas of two parts and acid leached. The results for smeared and nonsmeared were virtually identical. If one should be able to distinguish detection limit differences at these low levels (three to five times the detection limit), then the smearing technique used can be no more than 30% effective in removing boron from the final-finish surfaces.

It was thought that possibly the oiling treatments received after final finishing created a barrier to the water scrubbing treatments and thus reduced the effectiveness of the smearing. To test this hypothesis, mixtures of acetone and water or acetone, water, and a surfactant were used as the solvent medium for scrubbing the surface with polyvinylidene fluoride Millipore filters. Acetone and surfactant were added to help dissolve any residual oils. (The type of filter was changed to be compatible with the acetone.) Three boron coolant-machined parts, 5715, 5713, and 5692, were scrubbed on undisturbed portions of the IC with these solutions. The boron removed was still below the detection limit of ~8 ng/cm^2. Thus if a nondestructive method is needed in the future for determining these very low levels of boron residues on finished parts, additional development work will be required.

In summary, the boron residues on the final-finish machined parts were quite low. In each case the boron levels were close to the detection limits for the very sensitive ICP spectrometer. By acid etching, considered the most reliable of the techniques, the total boron residues were found to be 15 $\pm$ 3 ng/cm^2. The use of chips resulted in problems, but the net result of 19 $\pm$ 15 ng/cm^2 substantiates the acid etching results. The chip data indicate that the IC surfaces average somewhat more boron than found on the OC surfaces. Overall, this level of boron is not considered to be a problem for the processing done at the Rocky Flats Plant.

General Surface Contamination

General surface contamination was surveyed by secondary ion mass spectrometry (SIMS) and by electron spectroscopy for chemical analysis (ESCA). Inner and outer contours of all samples were analyzed with SIMS, and all inner contour surfaces were analyzed with ESCA. An Applied Research Laboratories (ARL) ion microprobe mass analyzer (IMMA) utilized a 20-keV N_2^+ primary ion beam for all SIMS analyses. The McPherson ESCA 36 photoelectron spectrometer used Al Kα radiation at 250 W (12.5 kV at 20 mA) for analyses. Just prior to insertion into either instrument, the disks were flushed with Freon to remove the surface oil that had been applied after cutting to improve storage.

SIMS Studies

All SIMS secondary-ion spectra in this report are normalized to the most intense peak in the spectrum. All negative ion spectra are normalized to O^-; positive ion spectra are normalized to UO^+ except for the mass spectrum in Fig. 3, in which the most intense peak is UO_2^+. Outer contour spectra tended to be more intense due to geometry effects of the curved surfaces.

Positive secondary-ion spectra from the mouth area of part 5715 (like Rocky Flats test parts) are shown in Figs. 3(a) through 4(c). A large number of elements are observed on these surfaces including H, Li, B, C, O, Na, Mg, Al, Si, P, Cl, K, Ca, Ti, Cr, Fe, Mn, Ni, Co, Cu, Zn, Sr, Ba, Pb, and U. In general, the spectra of the inside and outside surfaces were similar. There appeared to be a little more boron on the inside surface, which agreed with the chip data above. (For perspective, remember the measured boron levels averaged 29 ng/cm^2 on the IC and 11 ng/cm^2 on the OC. Also, compare the ESCA spectrum on the IC surface in Fig. 13, which shows only uranium, oxygen, carbon, and traces or minor peaks due to calcium and sulfur.)

Negative secondary-ion spectra show those elements that preferentially form negative ions. Figures 5 and 6 show the negative ion spectra from the OC and IC in the mouth area of part 5715. Both show considerable oxygen, chlorine, carbon, and fluorine on these surfaces. All the peaks above mass 40 are combination peaks formed from some of these four elements and possibly hydrogen or nitrogen. No significant differences in the spectra from the mouth, 45°, and pole areas were found. Thus, the secondary-ion spectra from the latter two areas are not included.

Figures 7(a) through 8(c) show the positive secondary-ion spectra from the OC and IC surfaces of standard treatment, boron coolant-machined sample 5713. These mass spectra are quite similar to those from part 5715. One difference, however, is the presence of silver, seen in Fig. 7(b). Silver was not seen on any of the other spectra from the 5715 or matching part 5692 coupons. As with part 5715, boron was slightly more intense on the IC surface.

The negative secondary-ion spectra from part 5713 are shown in Figs. 9 and 10. Again, oxygen, chlorine, carbon, and fluorine are the dominant negative peaks. The OH peaks are relatively higher and the chlorine, carbon, and fluorine peaks relatively lower on these standard treatment samples than on the samples like those sent to Rocky Flats. This difference probably reflects the additional time that the standard samples had to adsorb moisture and to oxidize.

The secondary-ion mass spectra from the surfaces of the perc-machined parts are similar to those of the boron coolant-machined parts. The positive secondary-ion mass spectrum from the 45° IC of part 5726 (standard treatment, perc-machined) is shown in Fig. 11. In comparing this spectrum with that of its counterpart from a boron-coolant surface (Fig. 8), it is observed that although the boron

Y-GA 86-952

counts

10^5

10^4

10^3

10^2

10^1

H   Li   B   CH   O   Ca^{+2} Mg Mg   Al   Si   Si   P   O$_2$ Cl   Ca   Ca   K   Ca   Ti   Cr   Cr   Fe   Mn   Fe   Ni   Co   Ni   Cu   Zn, TiO   Cu   Zn   Zn   FeO, CaO$_2$ Fe, CaO   F$_2$O   CaCl   Cu,Cl

Na   K

0   10   20   30   40   50   60   70   80

M/E

Fig. 3a. Positive mass spectrum from outer contour of part 5715, mouth area, mass range 0–80.

Y-GA 86-953

counts

10^3

10^2

10^1

Sr ^{235}U^{+2} Ba   BaO

80   90   100   110   120   130   140   150   160

M/E
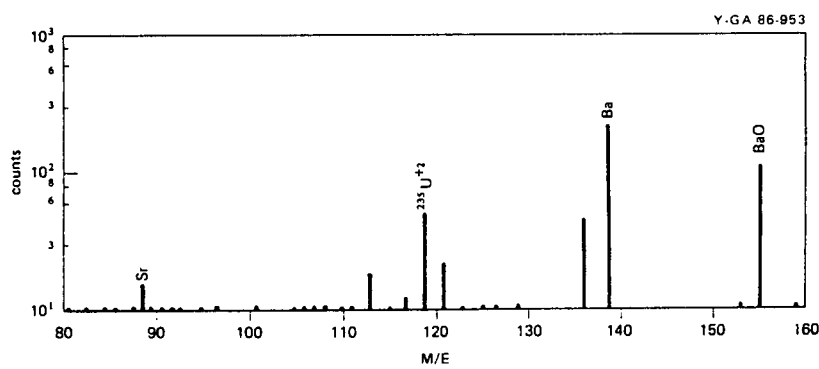
Fig. 3b. Positive mass spectrum from outer mouth contour of part 5715, mouth area, mass range 80–160.

Y-GA 86-954

counts

10^5

10^4

10^3

10^2

10^1

Pb   Pb ^{235}U ^{238}U ^{235}UO ^{238}UO   UC$_2$ UCN ^{235}UO$_2$ ^{238}UO$_2$ UCNO   UO$_3$

160   180   200   220   240   260   280   300   320

M/E
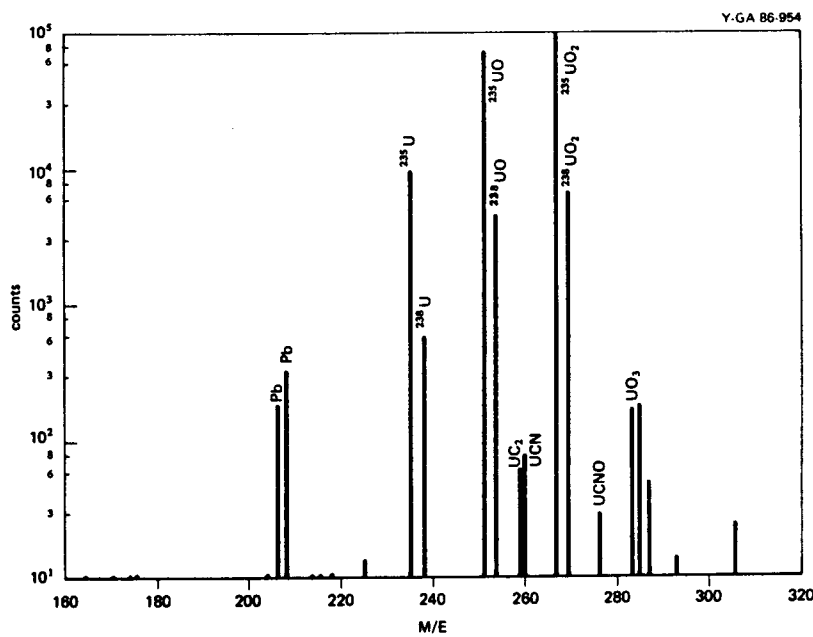
Fig. 3c. Positive mass spectrum from outer contour of part 5715, mouth area, mass range 160–320.

Fig. 4a. Positive mass spectrum from inner contour of part 5715, mouth area, mass range 0–80.
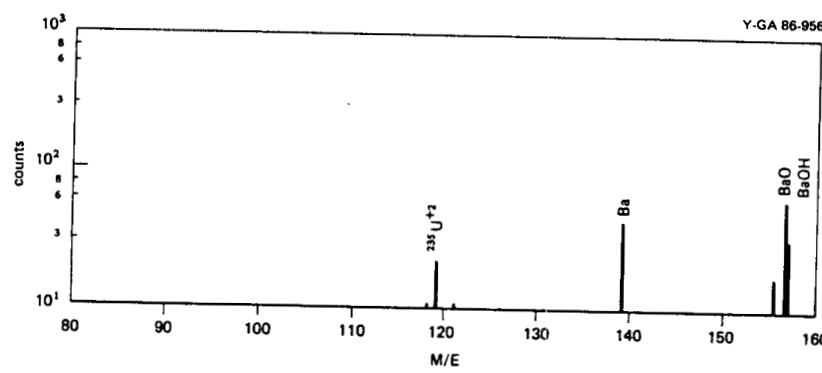

Fig. 4b. Positive mass spectrum from inner contour of part 5715, mouth area, mass range 80–160.
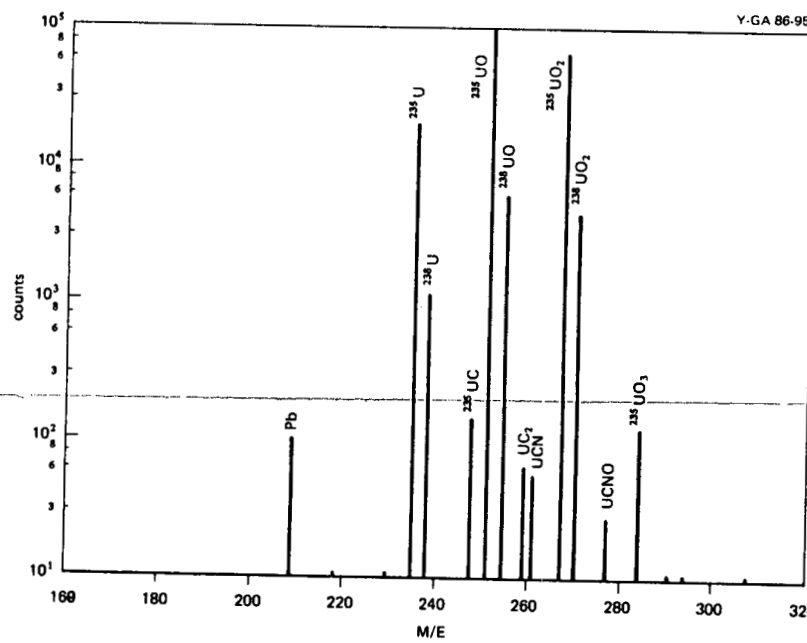

Fig. 4c. Positive mass spectrum from inner contour of part 5715, mouth area, mass range 160–320.

Y-GA 86-958
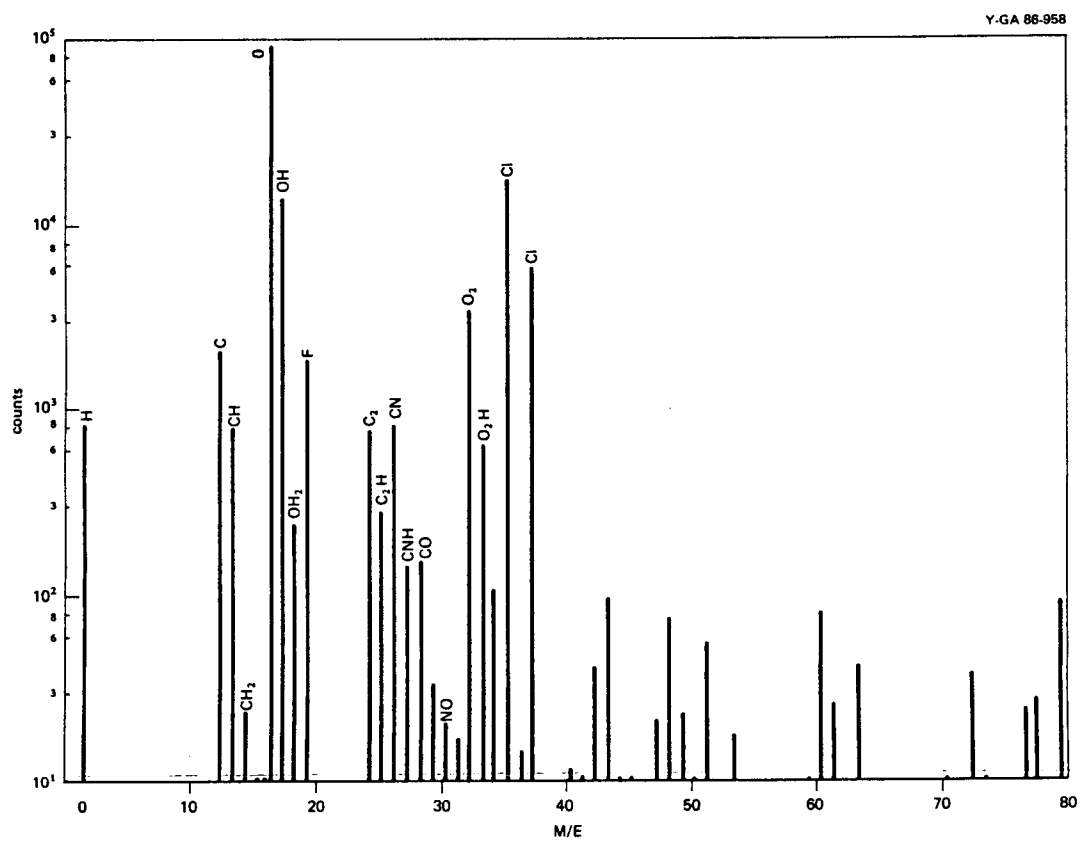
Fig. 5.   Negative mass spectrum from outer contour of part
5715, mouth area.

Y-GA 86-959
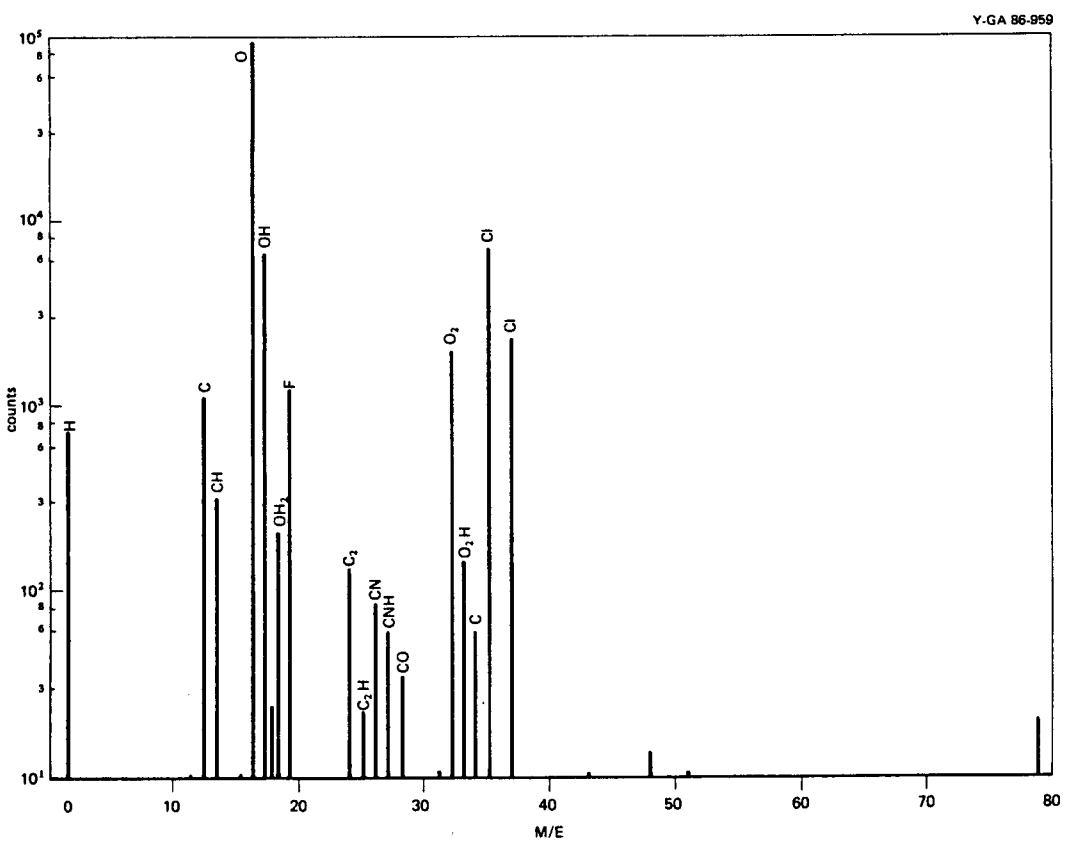
Fig. 6.   Negative mass spectrum from inner contour of part
5715, mouth area.

Y-GA 86-960
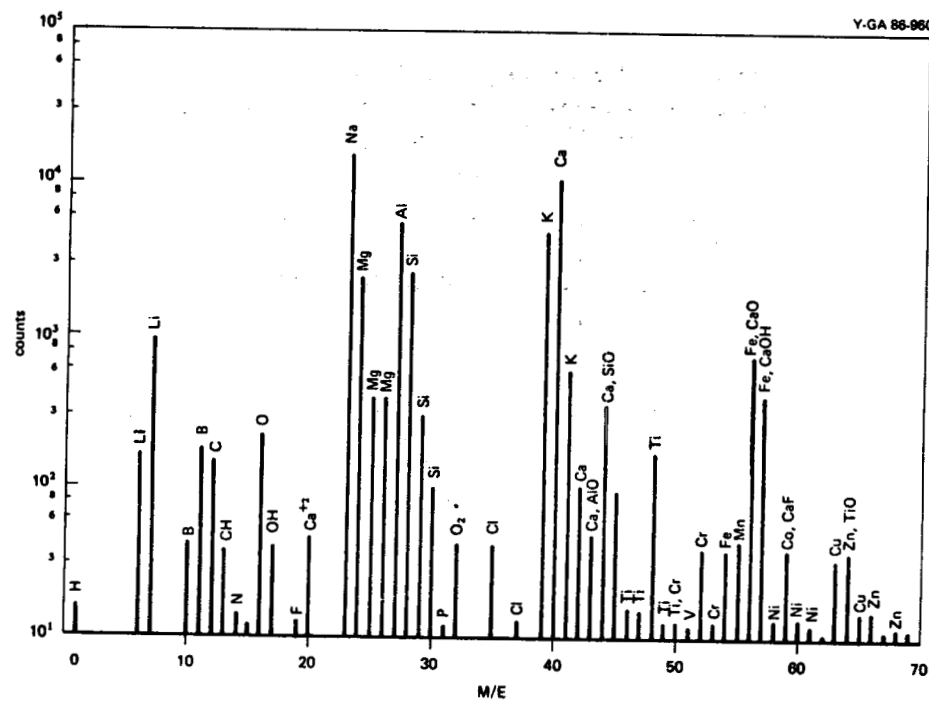
Fig. 7a. Positive mass spectrum from outer contour of part 5713, mass range 0–70.

Y-GA 86-961
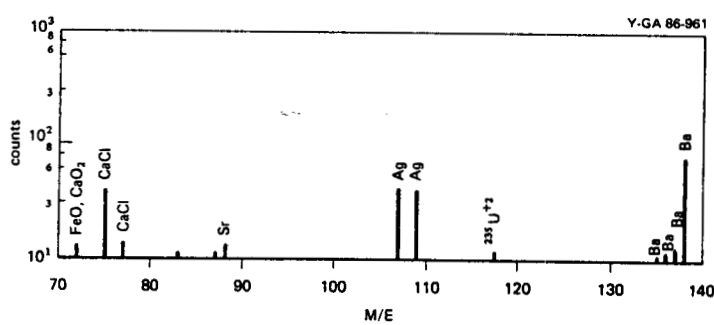
Fig. 7b. Positive mass spectrum from outer contour of part 5713, mass range 70–140.

Y-GA 86-962
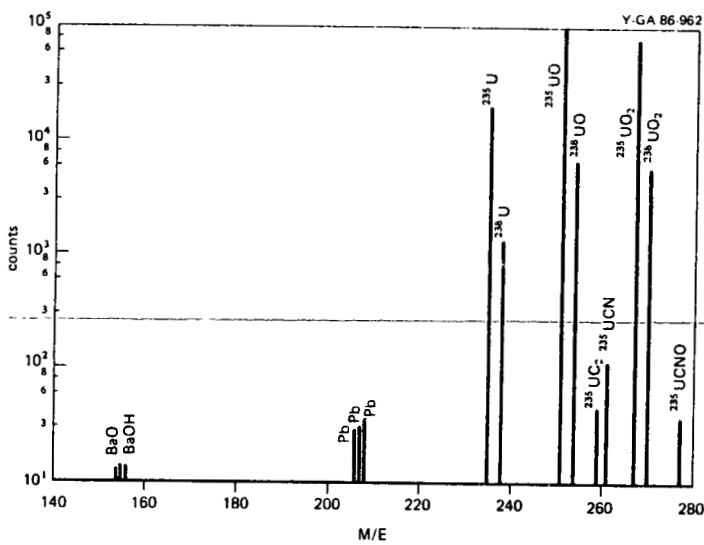
Fig. 7c. Positive mass spectrum from outer contour of part 5713, mass range 140–280.

17
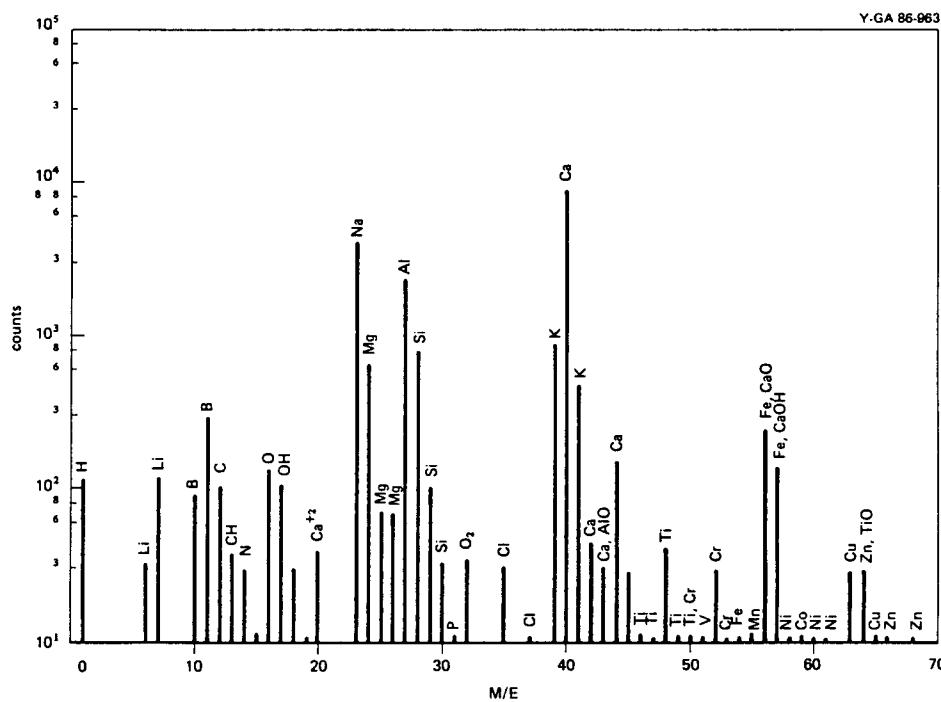
Fig. 8a. Positive mass spectrum from inner contour of part 5713, mass range 0–70.
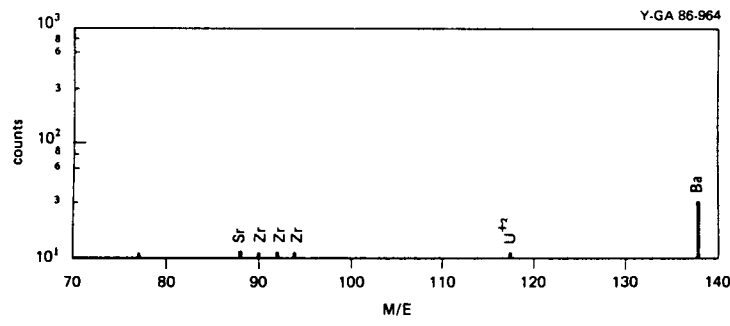
Fig. 8b. Positive mass spectrum from inner contour of part 5713, mass range 70–140.
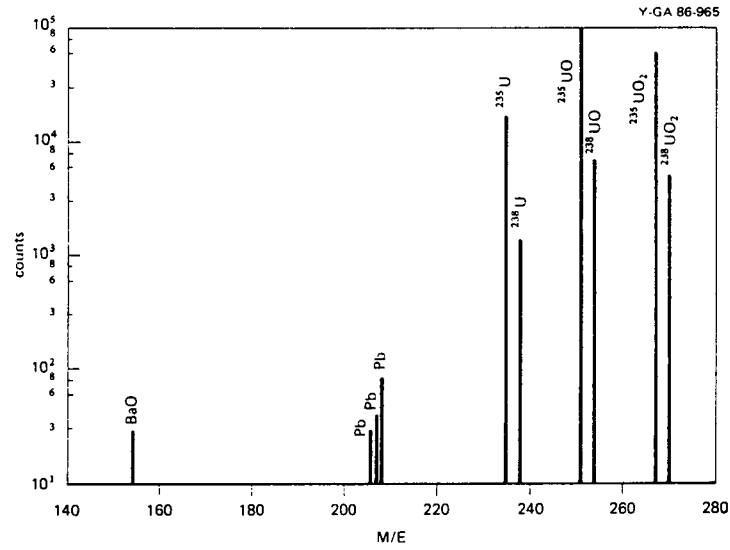
Fig. 8c. Positive mass spectrum from inner contour of part 5713, mass range 140–280.
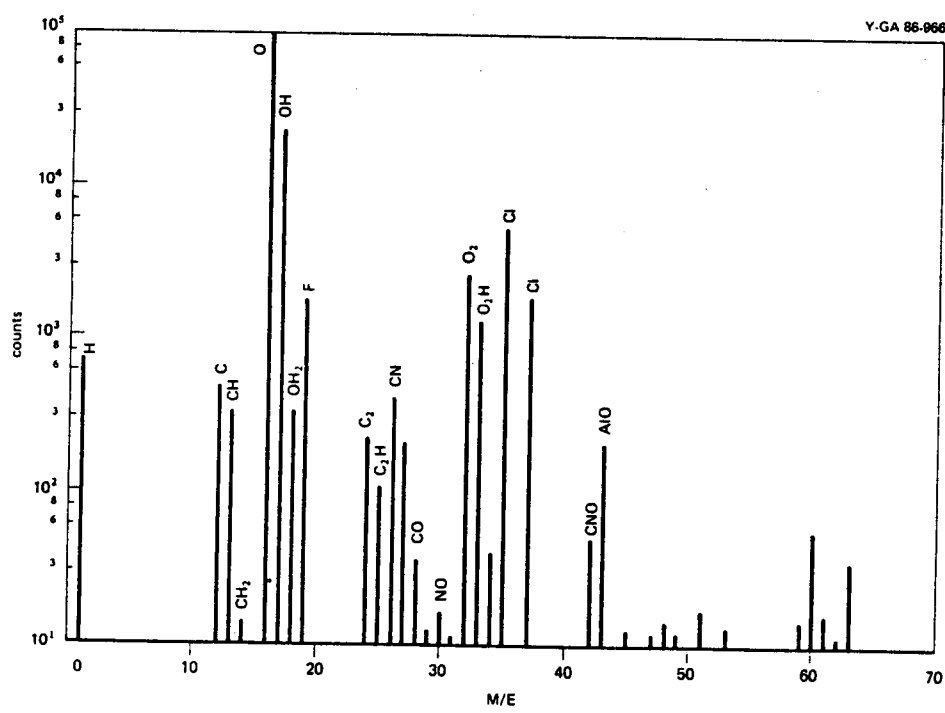
Fig. 9. Negative mass spectrum from outer contour of part 5713.
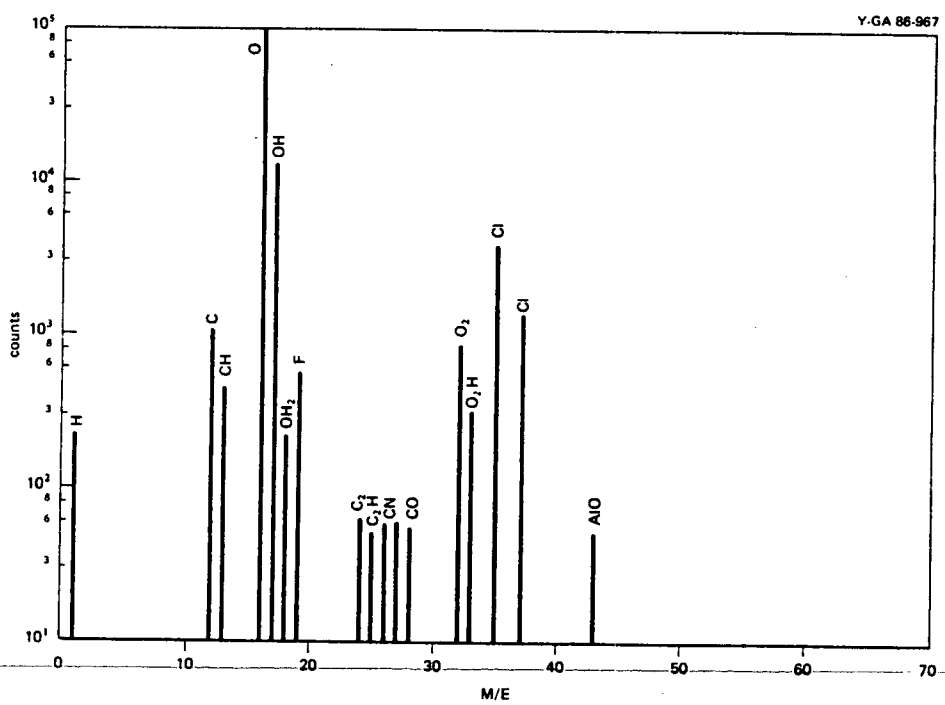
**Fig. 10. Negative mass spectrum from inner contour of part 5713.**
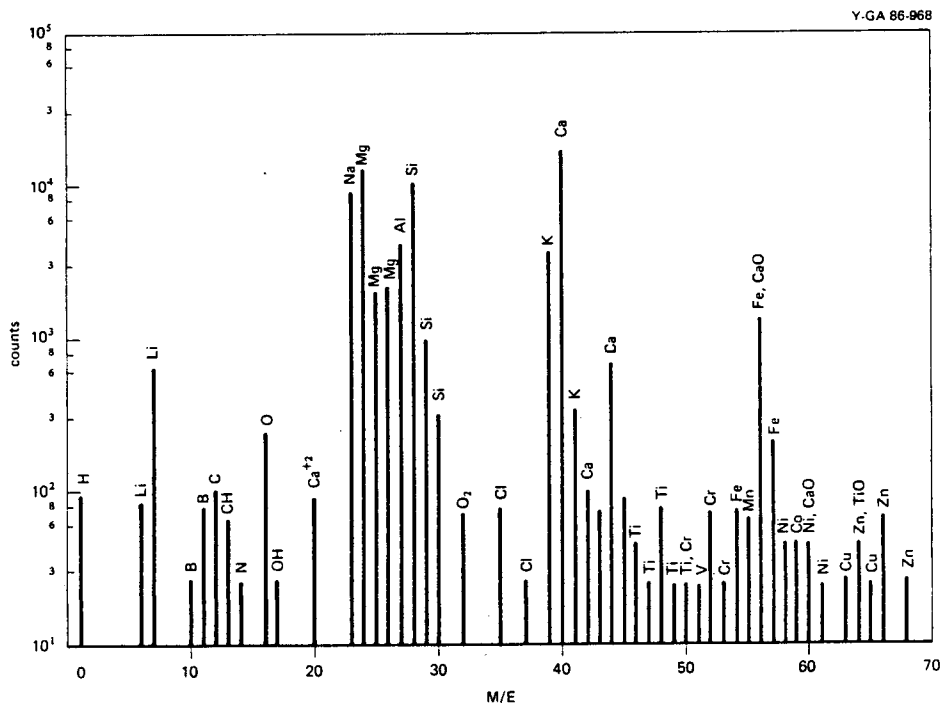
Fig. 11a. Positive mass spectrum from inner contour of part 5726, (perc machined) 45° area, mass range 0–70.
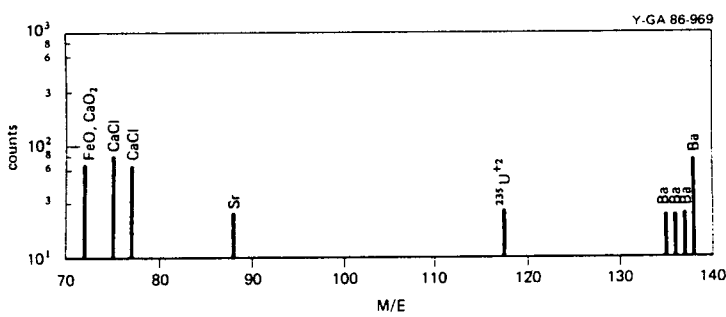

Fig. 11b. Positive secondary-ion mass spectrum from inner contour of part 5726, mass range 70–140.
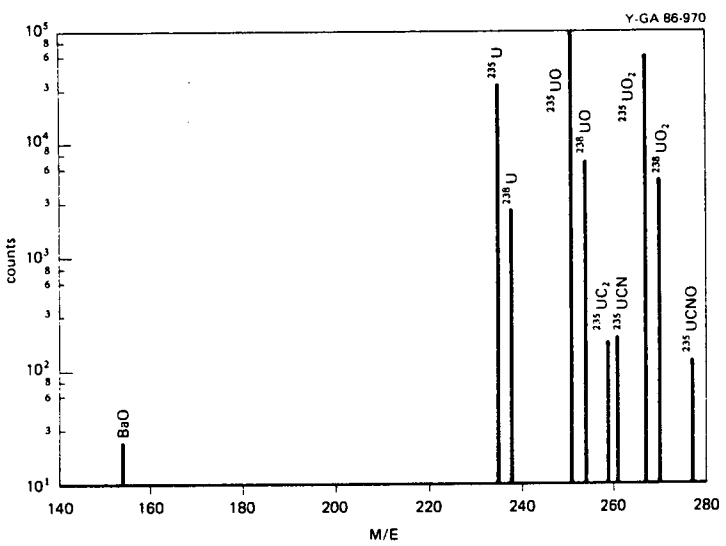

Fig. 11c. Positive mass spectrum from inner contour of part 5726, mass range 140–280.

level is lower in this spectrum, it is not absent. Chlorine is higher, and the general level of most peaks is a little higher with some exceptions, such as lead. Figure 12 shows the negative secondary-ion spectrum from the same part 5726 surface. This surface appears to have a little more chlorine but less carbon and OH than its counterpart shown in Fig. 10.

All other perc-cut surfaces are similar to these and are not shown to avoid redundancy. Likewise, the boron-coolant surfaces not shown are similar to the standard treatment surfaces shown in Figs. 7 through 10. Overall, the differences in surface contaminants between the perc-machined and the boron coolant-machined surfaces are not great. Some differences observed were greater boron, carbon, and OH on the boron-coolant parts and greater chlorine on the perc-coolant parts.

ESCA Studies

Qualitative ESCA spectra, representative of the first five distinct surface conditions listed in Table 2, are shown in Figs. 13 through 17. All of the qualitative spectra were similar, with major photoelectron peaks from uranium, oxygen, and carbon. Also, traces or very minor peaks from calcium and sulfur were observed in all spectra. In one or two cases, sodium from the boron coolant and chlorine from the perc coolant were observed at very low levels. Low concentrations of boron, even if present, could not be distinguished because of boron's small photoelectric cross section and also because it would be obscured by a much stronger $U(5p_{3/2})$ peak, which is within a few electron volts of the main $B(1s)$ peak.

The $O(1s)$, $U(4f)$, and $C(1s)$ spectra were obtained from the mouth, 45°, and pole disks representative of all seven surface conditions listed in Table 2. Little differences in the spectra were observed among mouth, 45°, and pole. All of the spectra from the same photoelectron level are similar. There is some variation in intensity of the peaks, but consistency of the binding energies indicates that the same species are present on all surfaces. The $O(1s)$ spectra show at least two distinct peaks that can be deconvoluted, using a Gaussian deconvolution routine, into peaks with binding energies of 531.6 ± 0.15 and 529.4 ± 0.06 eV ($\pm 1\sigma$) with a full width at half maximum (FWHM) ($\pm 1\sigma$) of 2.97 ± 0.16 and 1.67 ± 0.03 eV, respectively. Figures 18 and 19 compare the $O(1s)$ spectra on the boron coolant-machined and perc-machined disks, respectively, after the standard treatment (45 d) and after 6 months of storage (225 d). As storage time increases, the $O(1s)$ low-binding energy (LBE) peak decreases and the $O(1s)$ high-binding energy (HBE) peak increases for both coolants, but the changes are greater for the perc coolant. The $O(1s)$ LBE peak is associated with oxidic-type oxygen, while the $O(1s)$ HBE peak is attributed, tentatively, by most investigators to be a hydroxylic-type oxygen[1,2] and dependent on the surface preparation and history.

22
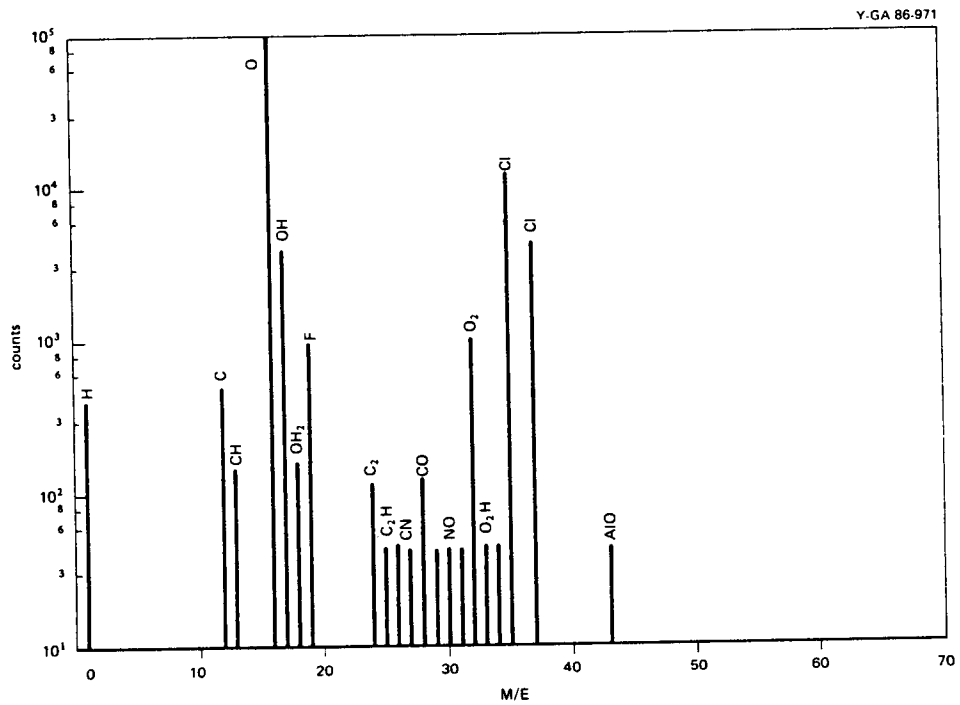
Fig. 12. Negative mass spectrum from inner contour of part 5726, (perc machined) 45° area.
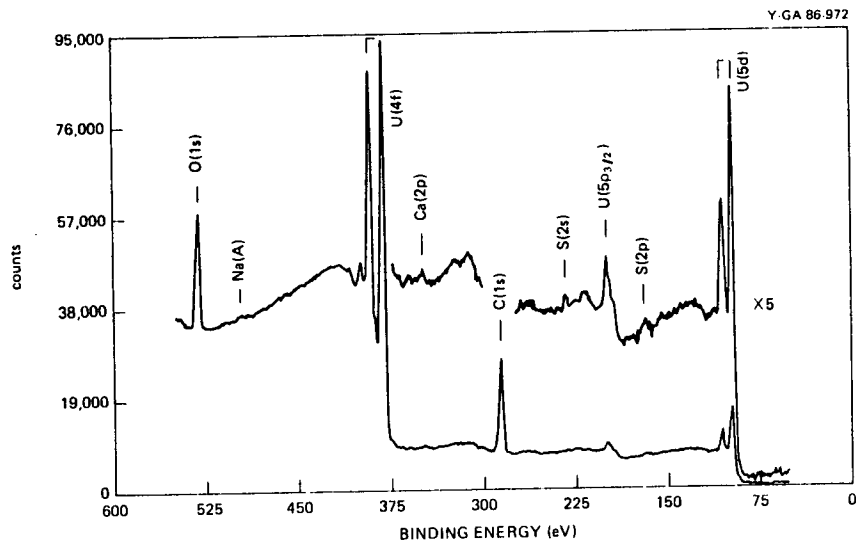
Fig. 13. Qualitative ESCA spectrum of enriched uranium machined with boron coolant— like Rocky Flats test parts.

Y-GA 86-973
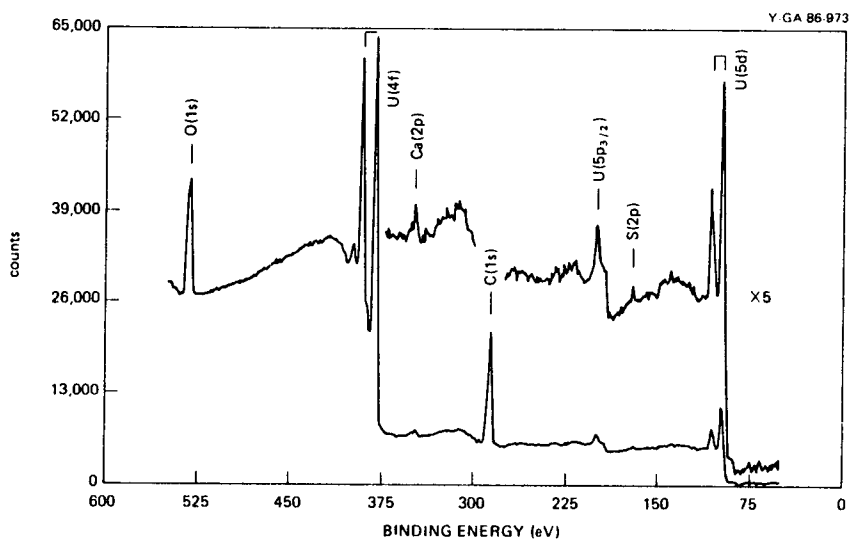
Fig. 14. Qualitative ESCA spectrum of enriched uranium machined with boron coolant—standard treatment.

Y-GA 86-974
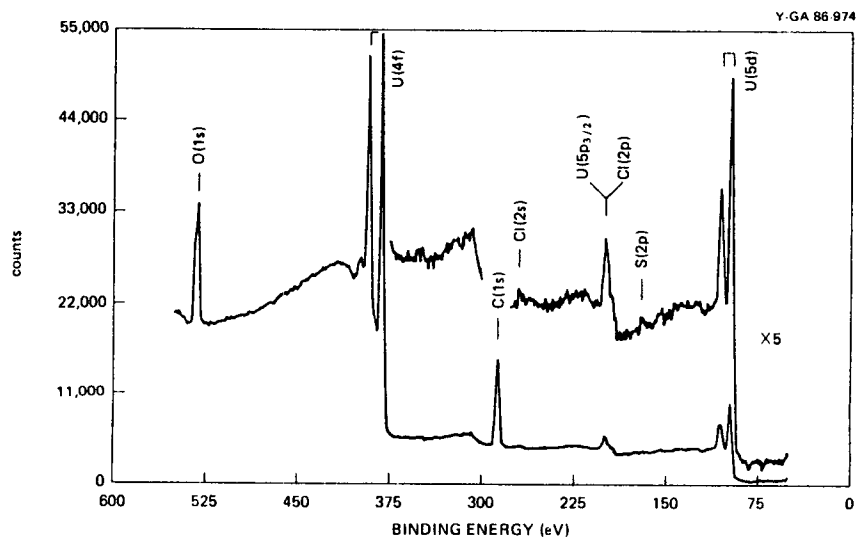
Fig. 15. Qualitative ESCA spectrum of enriched uranium machined with perc coolant—standard treatment.
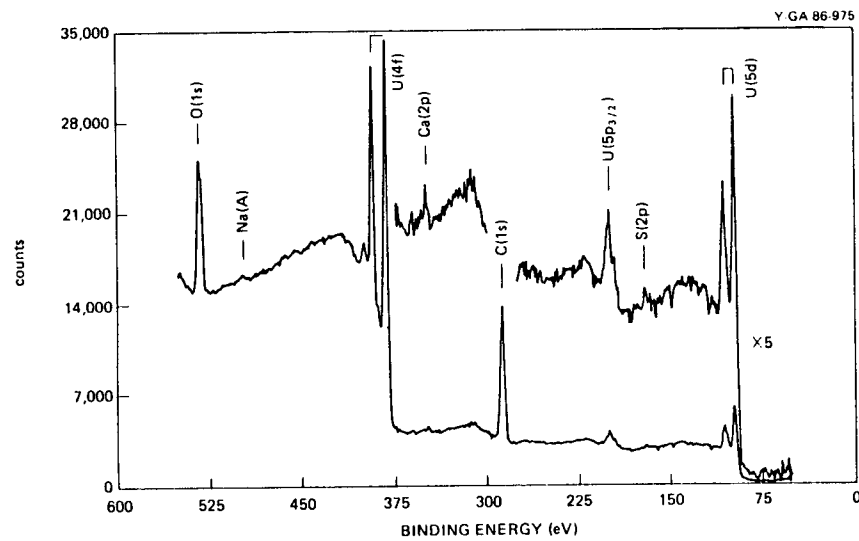
Fig. 16. Qualitative ESCA spectrum of enriched uranium machined with boron coolant—additional month storage in Rocky Flats bag.
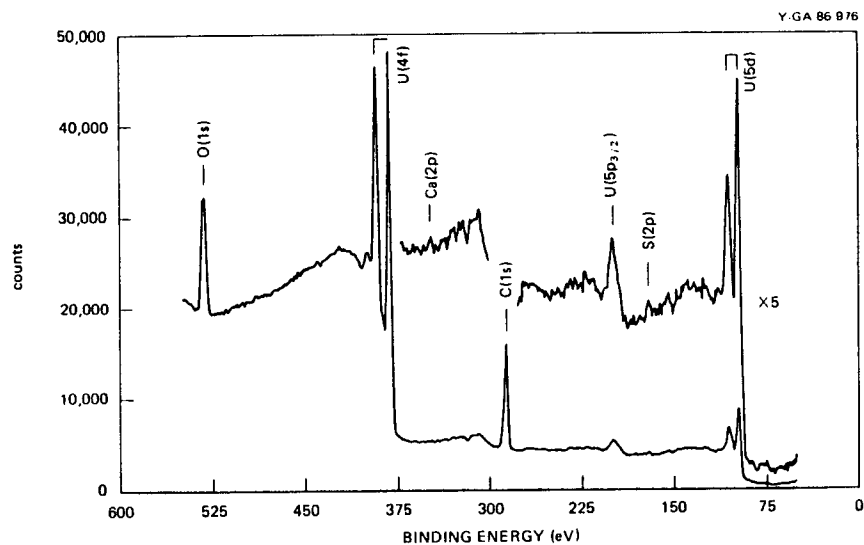

Fig. 17. Qualitative ESCA spectrum of enriched uranium machined with perc coolant—additional month storage in Rocky Flats bag.
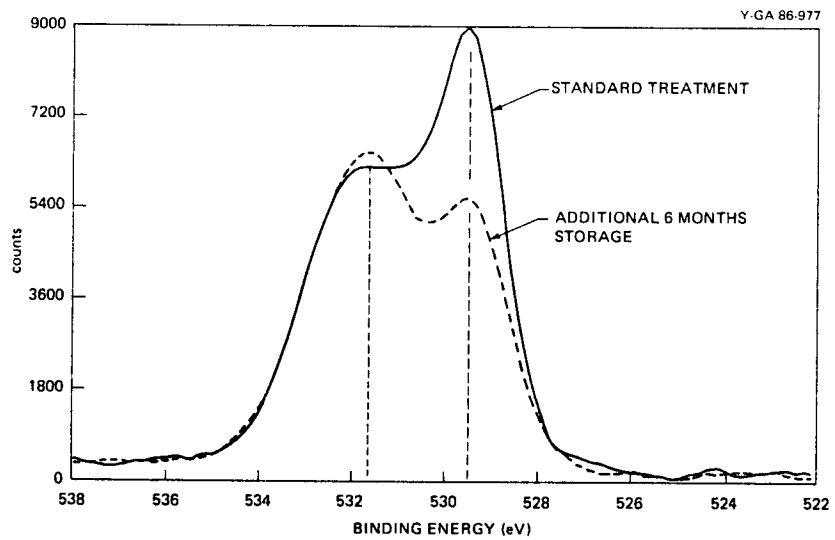
Fig. 18. O(1s) spectra from enriched uranium machined with boron coolant (pole position).
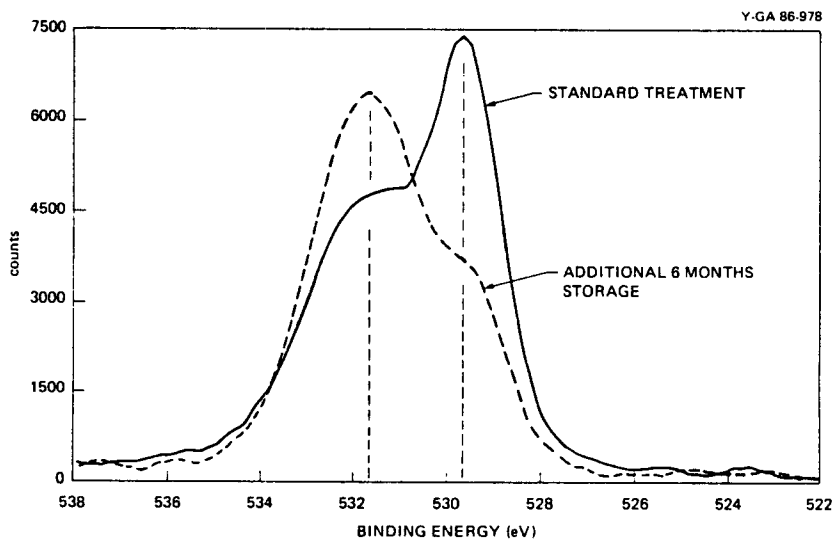

Fig. 19. O(1s) spectra from enriched uranium machined with perc coolant (pole position).

The binding energies of the U(4f) doublet are 390.4 ± 0.13 and 379.6 ± 0.13 eV with FWHM of 2.28 ± 0.11 and 2.24 ± 0.09 eV. Figures 20 and 21 compare the U(4f) spectra on the boron coolant-machined and perc-machined disks, respectively, after the standard treatment and after 6 months of storage. The U(4f) binding energies and the shake-up satellite structure on the HBE of the main peaks indicate uranium in the +4 oxidation state. As storage time increases, these spectra show a decrease in the U(4f) peaks and a shift toward higher binding energies, indicating a change toward higher oxidation states.

All binding energies are referenced to the C(1s) level at 284.6 eV and are the averages of 27 values. The C(1s) peaks for the boron and perc coolants are shown in Figs. 22 and 23, respectively. Because little change in the carbon spectra is seen with time, these figures illustrate the intensity changes that may be observed at different locations (pole, 45°, equator) on the parts. Table 6 gives atomic concentration ratios that show trends in the sample surface behavior. The relatively low standard deviations in the atomic ratio calculations show the consistency of the analyses within a particular surface condition. These data show several trends:

1. The O(1s)/U(4f) ratios for the boron-cut parts and the perc-cut parts are not significantly different.

2. The O(1s)/U(4f) ratio increases with storage time for both coolant-cut parts equally.

3. The C(1s)/U(4f) ratios for the boron-cut and for the perc-cut parts increase with storage time and are not significantly different.

4. The O(1s) HBE/O(1s) LBE ratio increases with storage time for both coolants, but the perc-cut ratio increases more than that for the boron-cut parts for storage times exceeding 64 d.

These trends were analyzed statistically using the F test. This test indicated that the increases in O(1s)/U(4f), C(1s)/U(4f), and O(1s) HBE/O(1s) LBE ratios were linear with respect to storage time. Differences between the three sample areas from either boron-cut or perc-cut parts were not statistically significant (see Appendix).

DETERMINATION OF OXIDE CORROSION LAYER THICKNESS

The IMMA was employed to determine the thickness or depth of the oxide corrosion layers that formed on the enriched uranium surfaces after each of the seven different conditions, as listed in Table 2. The layers were measured by sputtering at least two 31- by 39-µm rectangles on the surface of the IC and the OC of one coupon each from the mouth, 45°, and pole areas from each part. Examples of the secondary-ion depth profiles of O⁻ that were generated are shown in Figs. 24 and 25. Figure 24 shows a profile from part 5692 (standard treatment, boron coolant) with a relatively thin oxide, and Fig. 25 shows a profile from

Y-GA 86-979
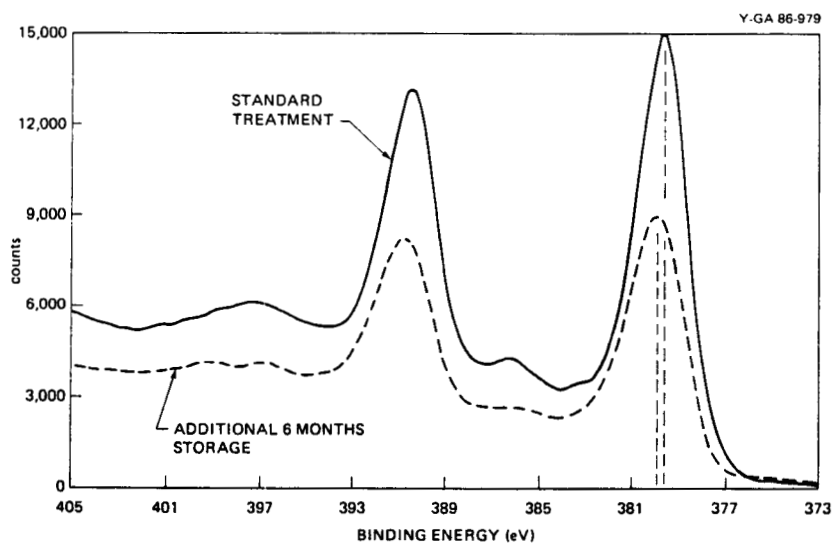
Fig. 20. U(4f) spectra from enriched uranium machined with boron coolant (pole position).
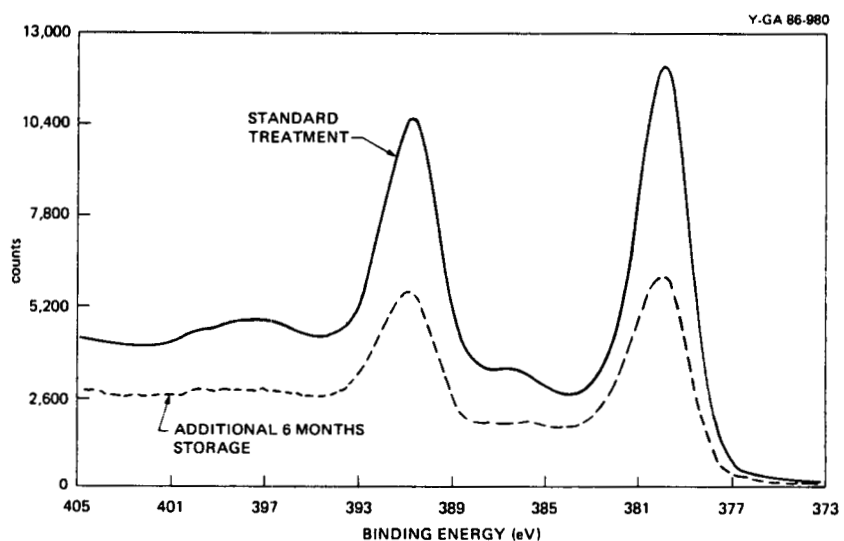
Y-GA 86-980

Fig. 21. U(4f) spectra from enriched uranium machined with perc coolant (pole position).
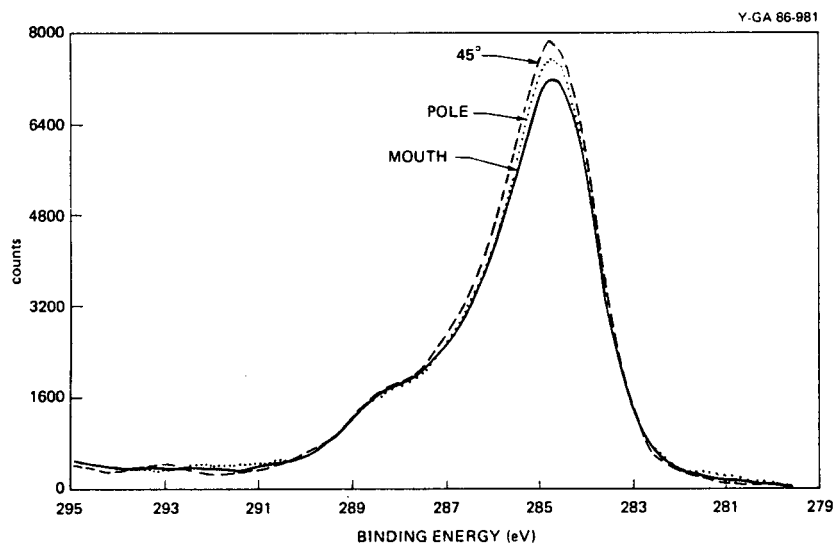
28

Y-GA 86-981

counts

8000

6400

4800

3200

1600

0

295   293   291   289   287   285   283   281   279

BINDING ENERGY (eV)

45°

POLE

MOUTH

Fig. 22.   C(1s) spectra from enriched uranium machined with boron coolant—additional 6 months storage in Rocky Flats bag.

Y-GA 86-982

counts

7500

6000

4500

3000

1500

0

295   293   291   289   287   285   283   281   279

BINDING ENERGY (eV)

POLE

45°

MOUTH
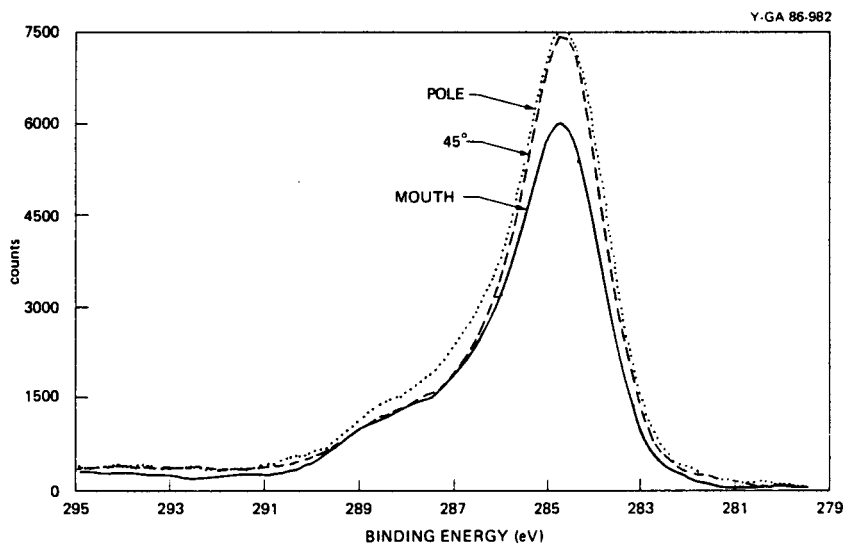
Fig. 23.   C(1s) spectra from enriched uranium machined   in perc coolant—additional 6 months storage in Rocky Flats bag.

Table 6. Summary of calculated atomic ratios from ESCA
determinations of relative atomic concentrations of
oxygen, uranium, and carbon on the boron- and perc
coolant-machined surfaces of enriched uranium

Days after machining	$\dfrac{O(1s)\ HBE}{O(1s)\ LBE}$	$\dfrac{O(1s)}{U(4f)}$	$\dfrac{C(1s)}{U(4f)}$
	Boron coolant		
30	1.34 ± 0.11	3.08 ± 0.47	5.42 ± 0.35
45	1.40 ± 0.15	3.60 ± 0.27	5.45 ± 0.67
75	1.94 ± 0.26	4.10 ± 0.32	6.88 ± 0.54
225	3.64 ± 1.39	6.05 ± 1.10	10.97 ± 2.75
	Perc coolant		
45	1.44 ± 0.18	3.43 ± 0.09	4.32 ± 0.45
75	1.62 ± 0.19	3.70 ± 0.29	5.23 ± 0.48
225	6.10 ± 1.52	6.47 ± 0.70	14.11 ± 3.87
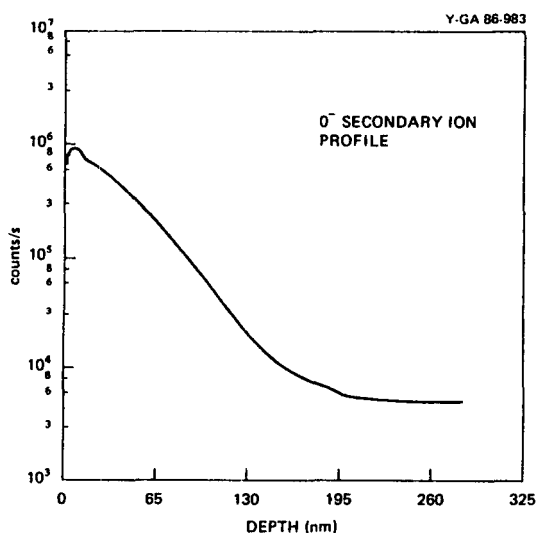
Fig. 24. Oxygen depth profile
on standard treatment, sample 5692,
boron coolant.

30

Y-GA 86-984

O⁻ SECONDARY ION PROFILE
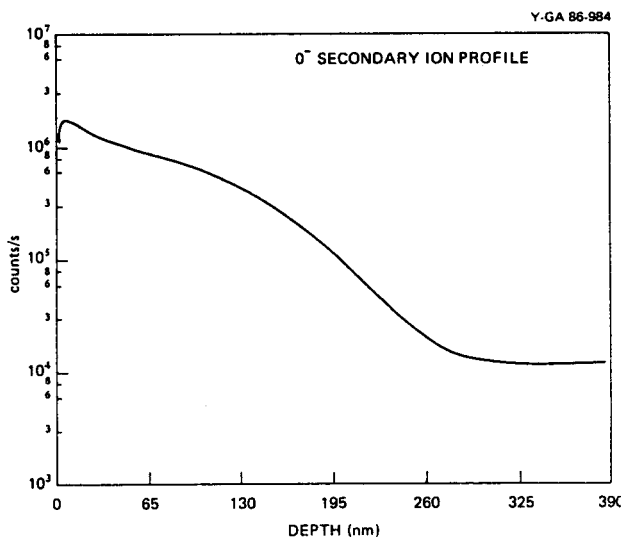
Fig. 25. Oxygen depth profile on standard plus 1 month storage, sample 5730, perc coolant.

part 5730 (perc coolant) which was stored for 1 month in a Rocky Flats bag after final processing. These profiles are of typical areas on these samples. The oxide depth measurements were calibrated by measuring sputtered craters with a surface profiler and by comparing them with ion implantation profiles determined by a nuclear reaction method.

Statistical analyses of variance (see Appendix) indicated that there are statistically significant differences in oxide depths at various locations and between the perc and boron coolant-machined shown graphically in Figs. 26 and A.4. The numbers of IC and OC are the averages of thicknesses measured on typical surfaces. On most of the samples, isolated pitted areas had much greater oxide thickness. The maximum, local, pitting thickness measured on each set is also shown in Table 7. These are not typical but do show that some small spots of severe corrosion are common on enriched uranium surfaces, particularly if the storage time exceeds 1 month after machining. The photomicrographs in the next section illustrate this point. Note that not all pits were measured; some pits deeper than those listed could exist.

Table 7 shows that as storage time after machining increases, the oxide thickness increases. The oxide depth on the perc-cut parts increased linearly and essentially equally on both the IC and OC at a rate of 1.6 nm/d. The oxide growth on the boron-cut parts, however, decreased from its initial linear rate and was greater on the OC than on the IC. A plot of these results is shown in Fig. 26. The statistical analyses indicated that one linear regression line could be used to fit

Table 7. Summary of IMMA determinations of oxide depth on the boron coolant–machined and perchloroethylene coolant-machined surfaces of enriched uranium

Part	Days after machining	Depth (nm)			Grand average	Maximum local pitting
		Average IC	Average OC	Average IC + OC		
Boron coolant machined						
5715	30	68 ± 37	59 ± 22	64 ± 28	64 ± 28	
5713	45	79 ± 11	115 ± 24	97 ± 26		
	45				101 ± 22	360
5692	45	97 ± 11	119 ± 23	106 ± 18		
5720	75	139 ± 21	162 ± 74	151 ± 50		
	75				163 ± 41	1130
5722	75	159 ± 28	192 ± 16	176 ± 27		
5727	225	329 ± 71	217 ± 104	273 ± 100	273 ± 100	~2000
Perc coolant machined						
5725	45	113 ± 20	124 ± 13	119 ± 16		
	45				114 ± 18	1400
5726	45	97 ± 23	122 ± 6	111 ± 20		
5730	75	178 ± 16	190 ± 33	184 ± 24		
	75				168 ± 31	1040
5733	75	159 ± 46	139 ± 19	152 ± 30		
5739	225	416 ± 30	394 ± 44	406 ± 38		
	225				414 ± 41	~2000
5740	225	447 ± 44	392 ± 17	423 ± 44		

all the data from the perc coolant-machined parts and that a second linear regression line could be used to fit all the data from the boron coolant-machined parts. This results in a slope or linear oxide growth rate of 1.0 nm/d for the boron-cut parts and 1.6 nm/d for the perc-cut parts. If these rates remain unchecked, spalling of oxide from the surface could be expected in ~1000 d after machining for the boron-cut parts and ~600 d for the perc-cut parts when the oxide reaches 1 μm in thickness.

This study of oxide growth on enriched uranium parts in a normal environment showed that boron coolant-machined surfaces oxidized at significantly lower rates than the perc coolant-machined surfaces.
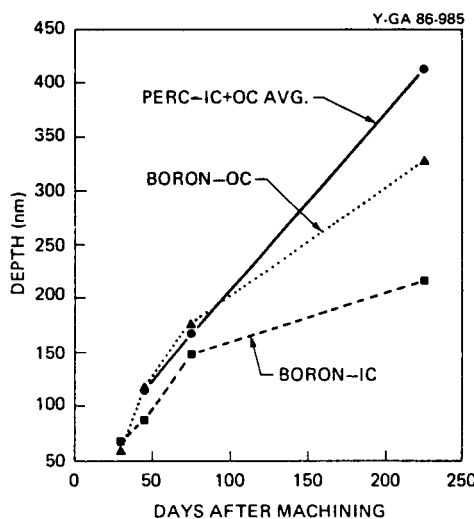
Fig. 26. Oxide growth on
perc- and boron-cut parts.

## SURFACE MORPHOLOGY AND LOCAL CORROSION

The scanning electron microscope (SEM) was utilized to survey both the IC and OC of all coupons. The same samples used in the IMMA analyses were used for the SEM work. The coupons were rinsed in Freon 113 just prior to the SEM analysis. A series of photomicrographs ranging in magnification from 100X to 3000X were made from a representative area of each coupon.

Corrosion pits were found on all surfaces examined, with the smallest number observed on the specimens like those sent to Rocky Flats (exposed to Y-12 environment for 30 d after final machining). The lengths of the pits ranged from less than 2 μm to greater than 20 μm. The pits were randomly dispersed, both individually and in groups. Except for the Rocky Flats-type coupons, all coupons regardless of their location or coolant used showed approximately the same degree of pitting. Also randomly dispersed were areas where the oxide growth pattern could be observed.

The various types of pitting and oxide growth patterns can be seen in Figs. 27 through 40. The highest magnification (3000X) photomicrograph in each figure shows either the detail of the pitting or the oxide growth. The relative sizes of the pits can be compared in the 1000X views, while the 300X photomicrographs, show the distribution of the pits in the same area. Figures 41 and 42 compare (at 1000X) the surface morphologies vs time after final machining for the boron-cut parts and the perc-cut parts, respectively.
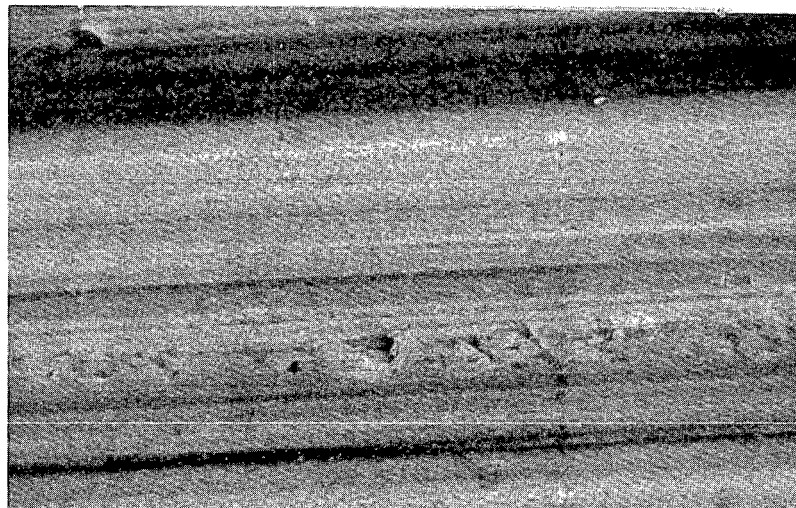
(a)
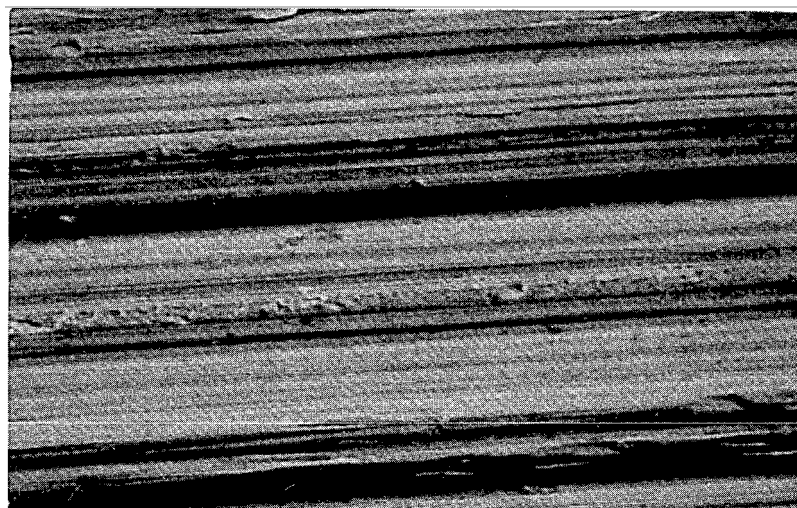
(b)
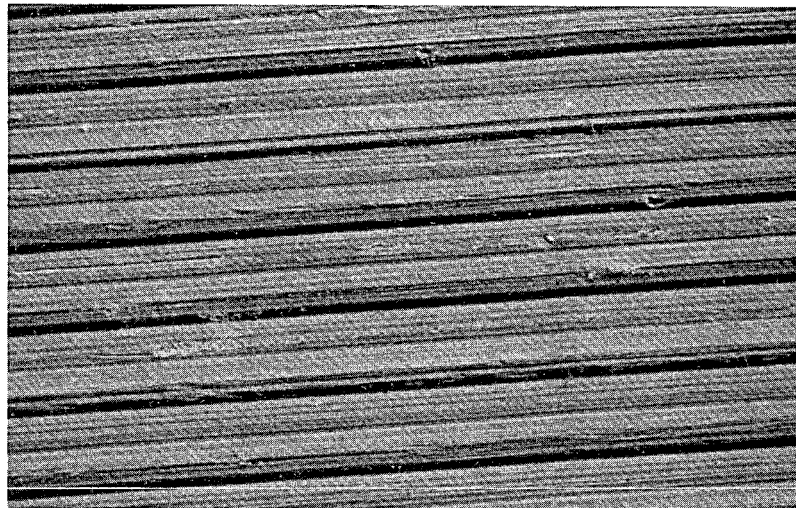
(c)

Fig. 27. Pitting and oxide growth patterns of boron coolant-machined part 5715 shown 30 d after final machining on the IC at 45°. Magnification: (a) 3000X, (b) 1000X, (c) 300X.

33
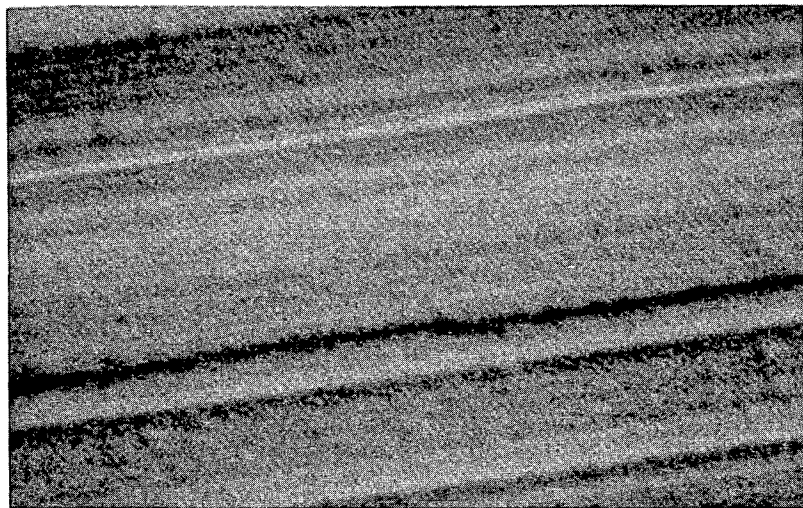
(a)
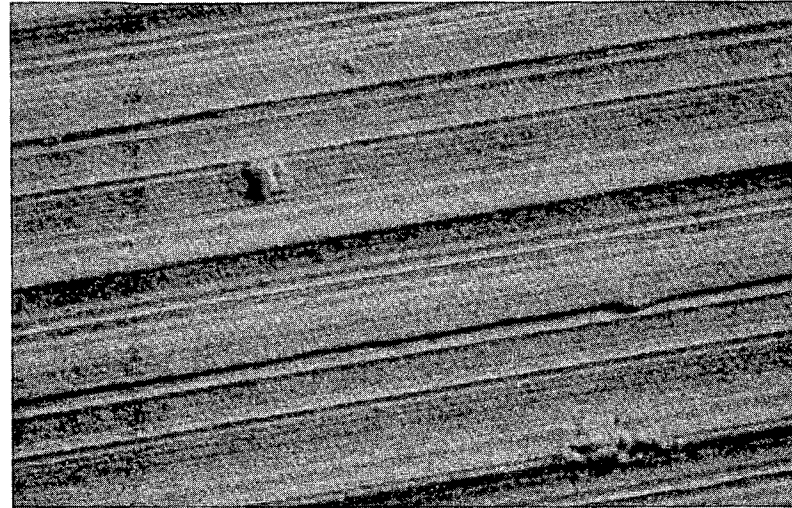
(b)
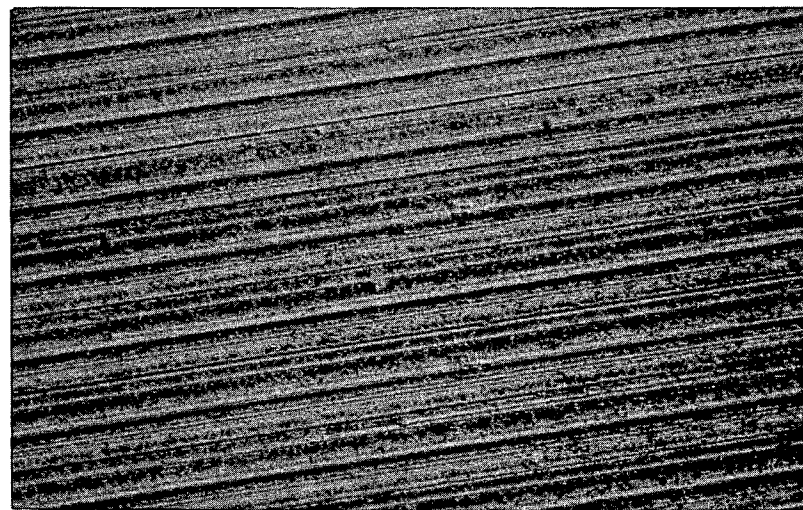
(c)

Fig. 28. Pitting and oxide growth patterns of boron coolant-machined part 5715 shown 30 d after final machining on the OC at the pole. Magnification: (a) 3000X, (b) 1000X, (c) 300X.
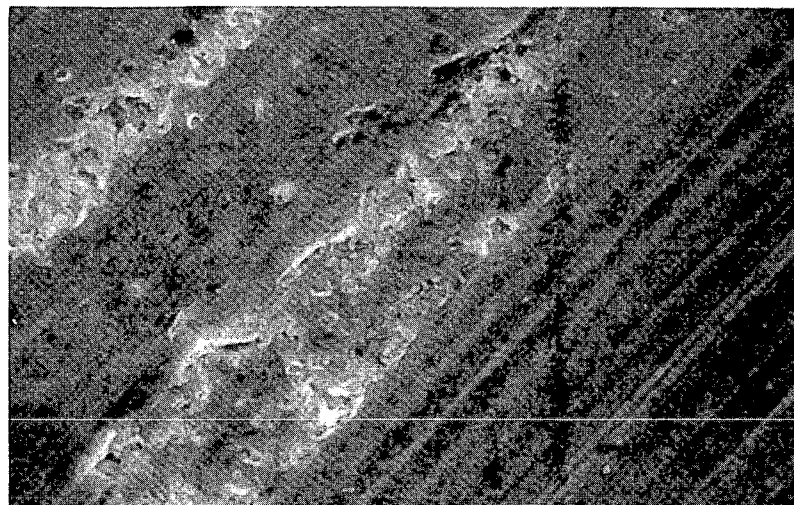
(a)
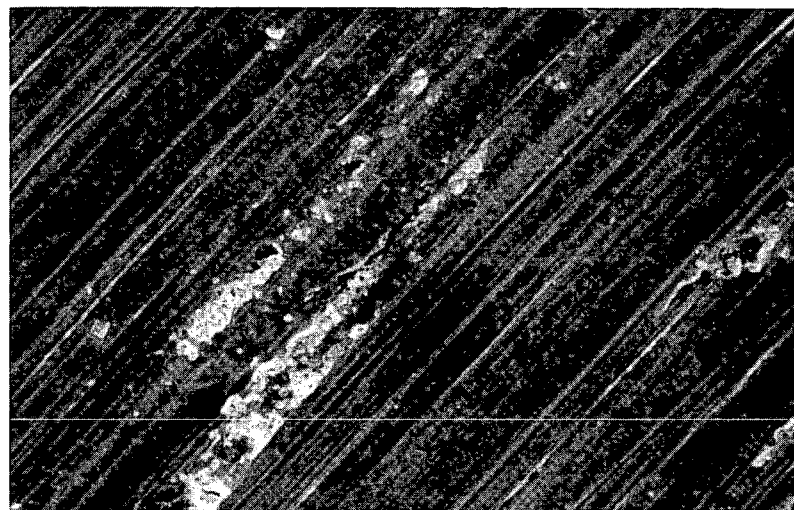
(b)
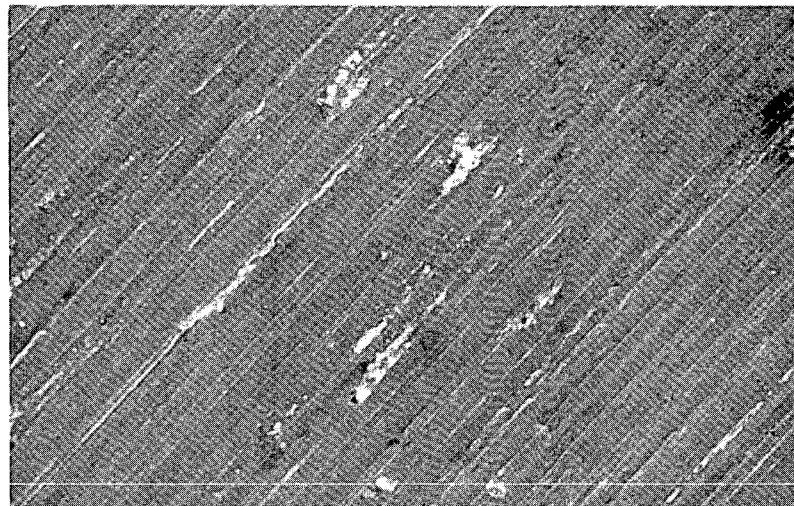
(c)

Fig. 29. Pitting and oxide growth patterns of boron coolant-machined part 5692 shown 45 d after final machining on the IC at 45°. Magnification: (a) 3000X, (b) 1000X, (c) 300X.
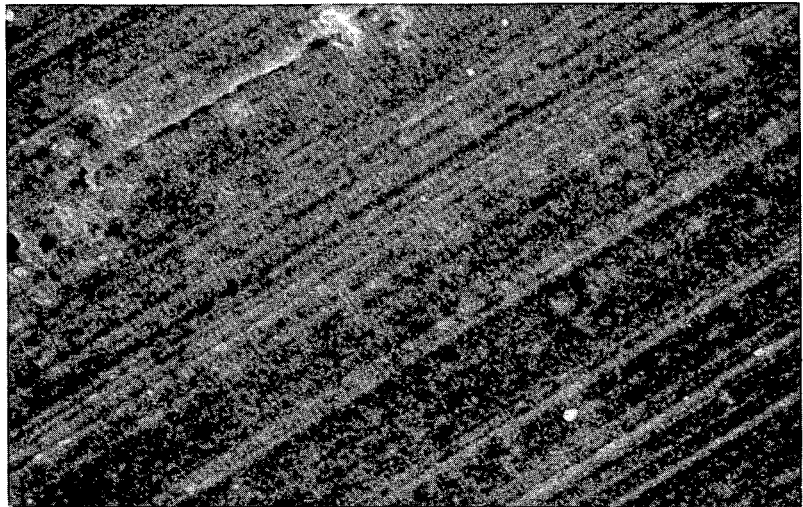
(a)
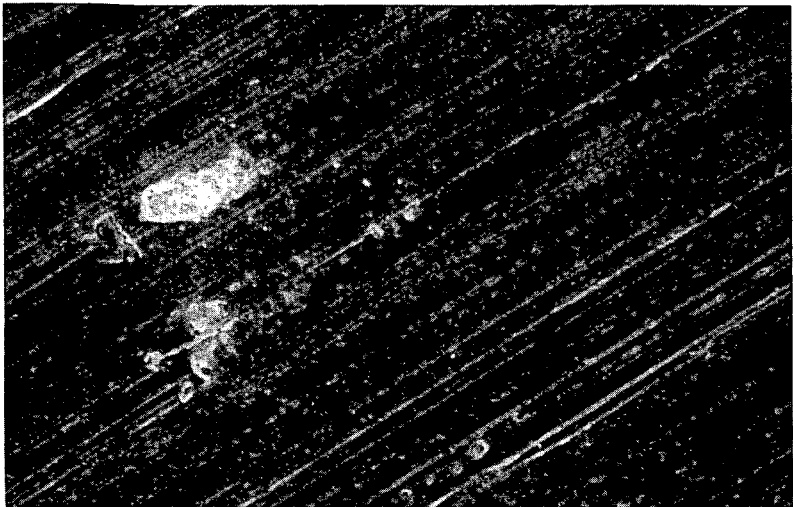
(b)
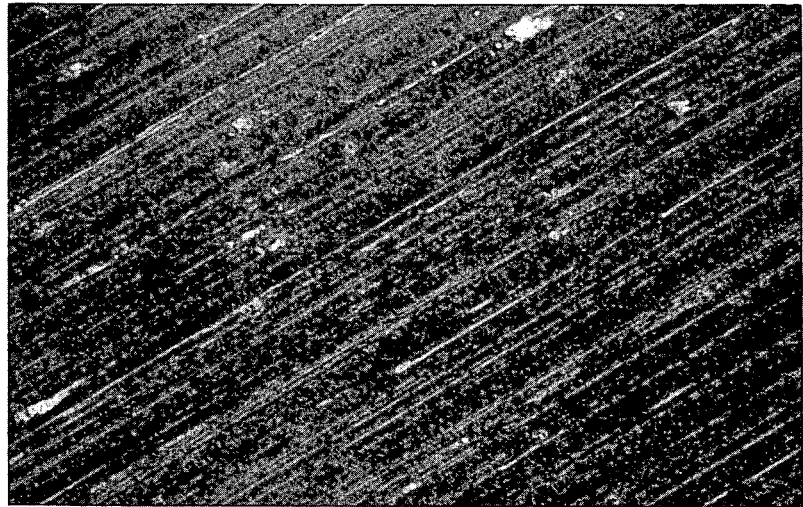

(c)

Fig. 30. Pitting and oxide growth patterns of boron coolant-machined part 5713 shown 45 d after final machining on the OC at the mouth. Magnification: (a) 3000X, (b) 1000X, (c) 300X.
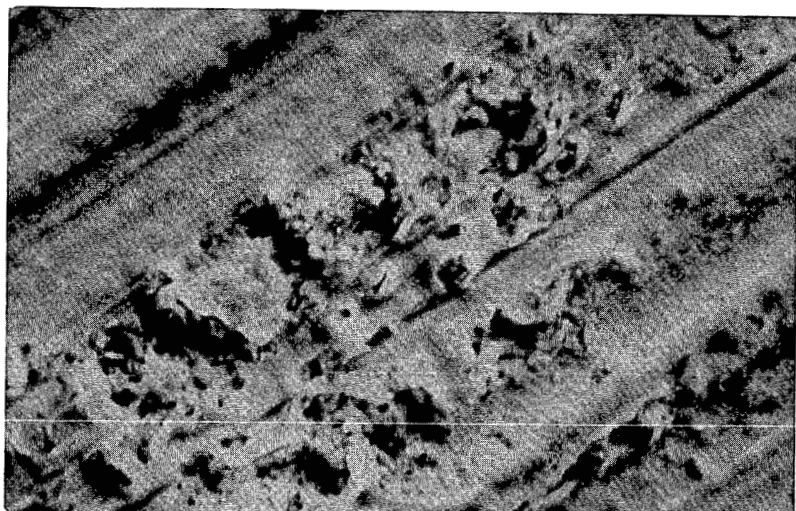
(a)
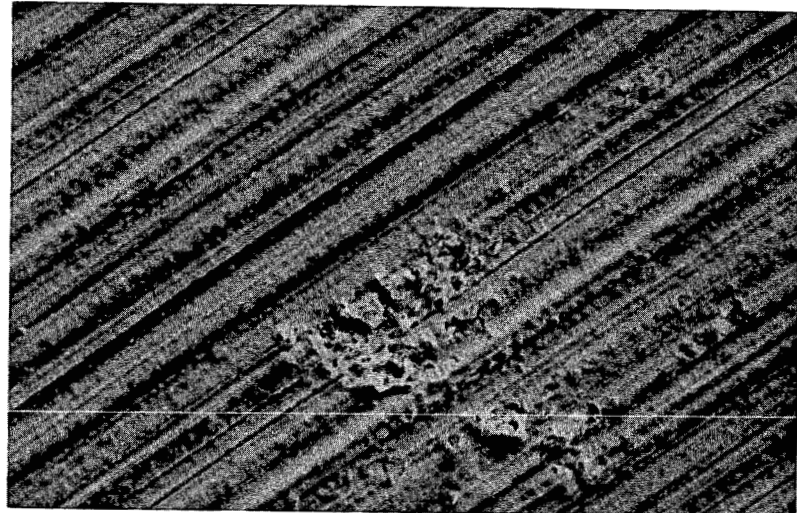
(b)
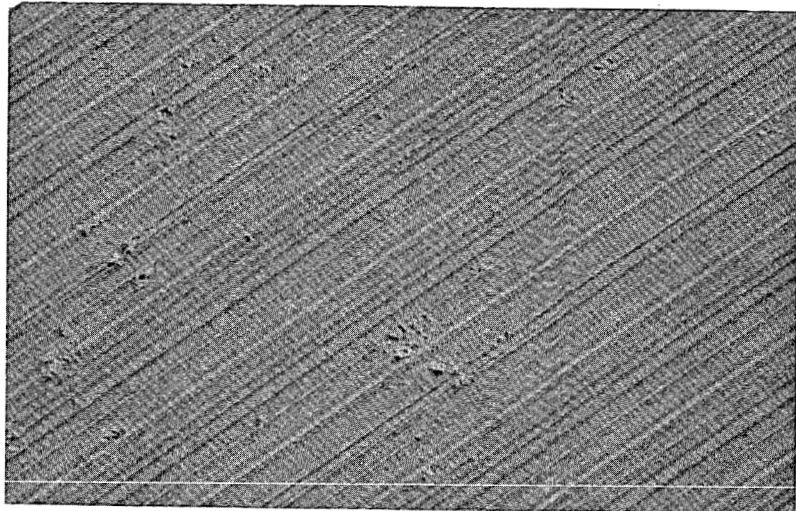
(c)

Fig. 31. Pitting and oxide growth patterns of boron coolant-machined part 5720 shown 75 d after final machining on the IC at the mouth. Magnification: (a) 3000X, (b) 1000X, (c) 300X.
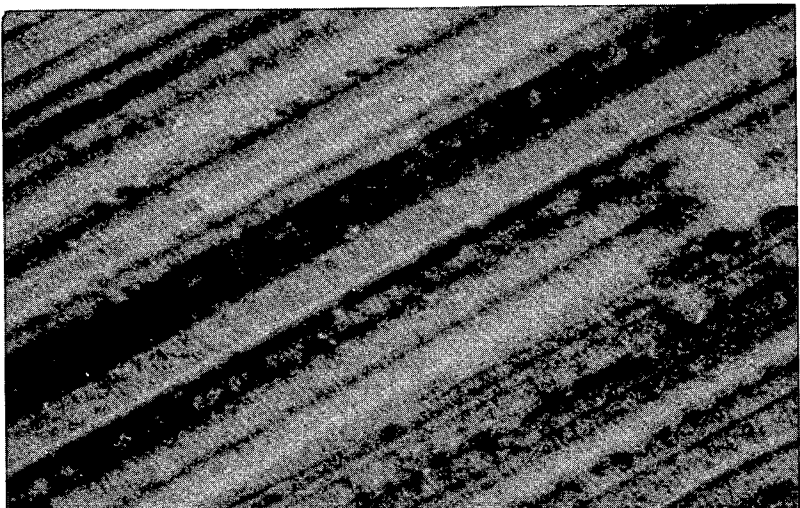
(a)
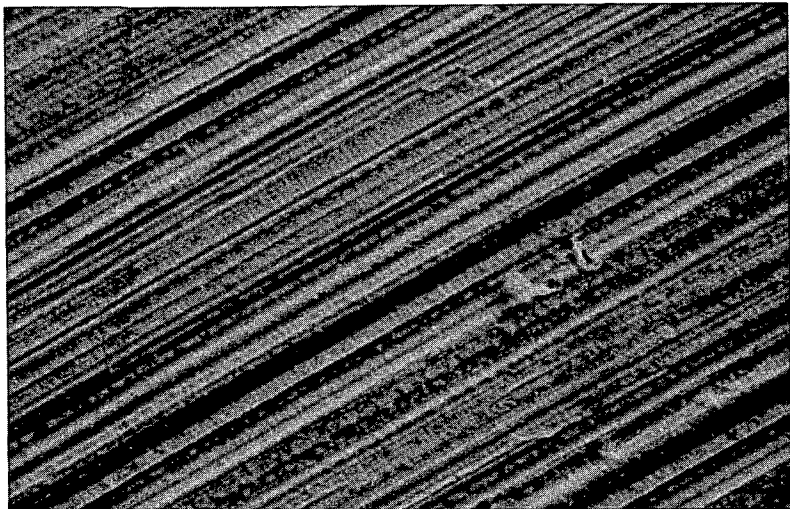
(b)
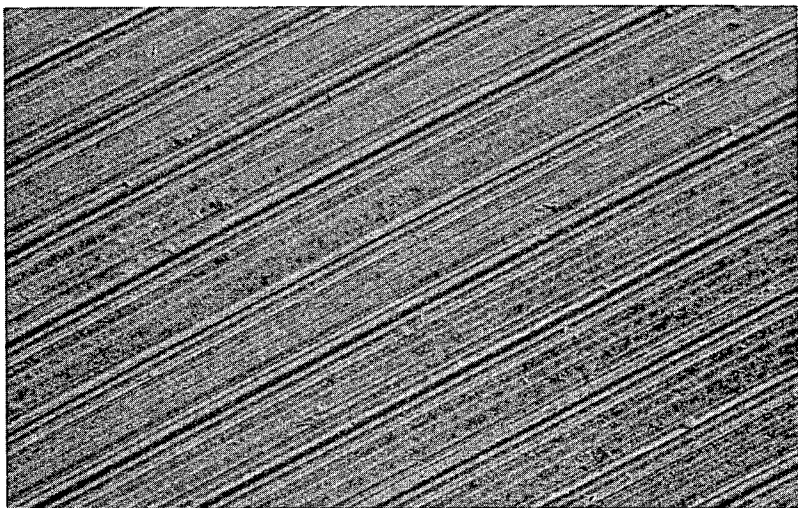
(c)

Fig. 32. Pitting and oxide growth patterns
of boron coolant-machined part 5722 shown 75 d
after final machining on the OC at the pole.
Magnification: (a) 3000X, (b) 1000X, (c) 300X.
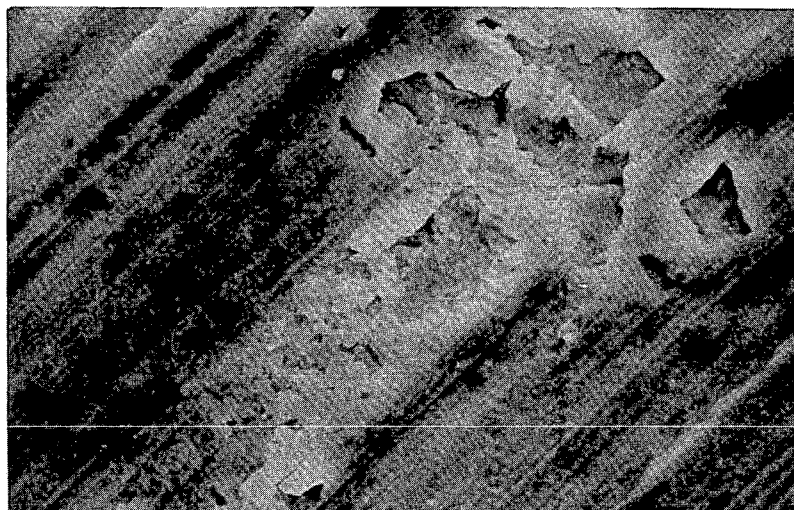
(a)
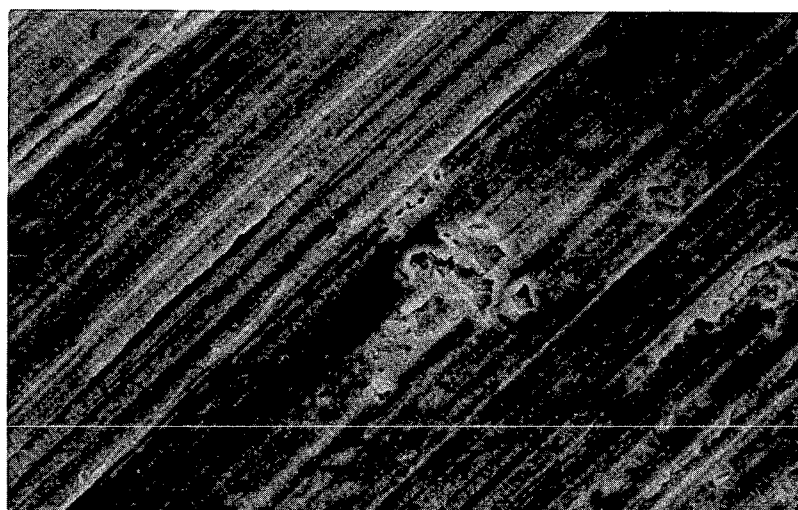
(b)
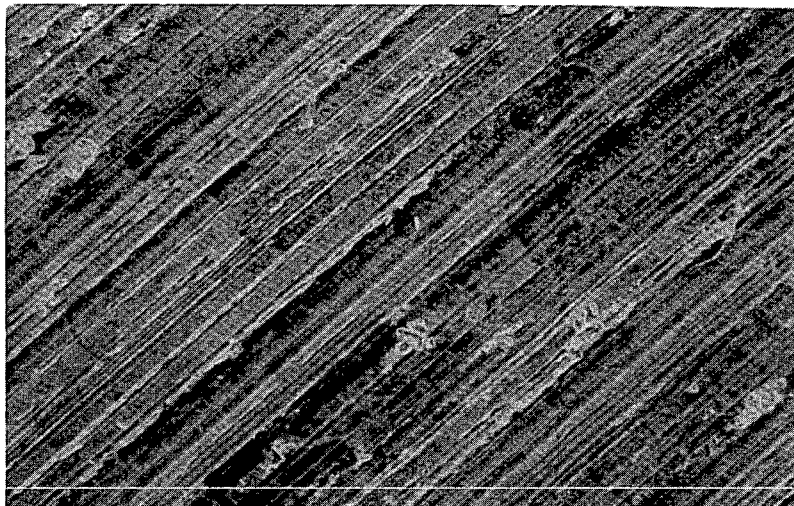
(c)

Fig. 33.   Pitting and oxide growth patterns of boron coolant-machined part 5727 shown 225 d after final machining on the IC at 45°. Magnification: (a) 3000X, (b) 1000X, (c) 300X.
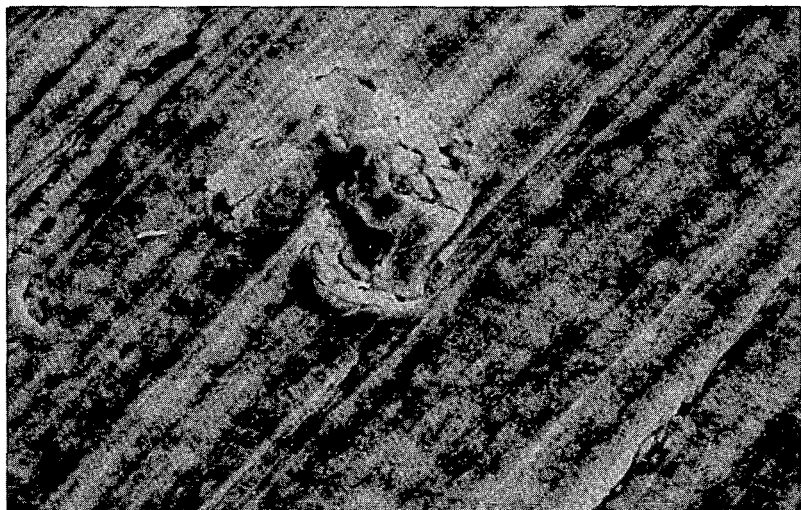
(a)
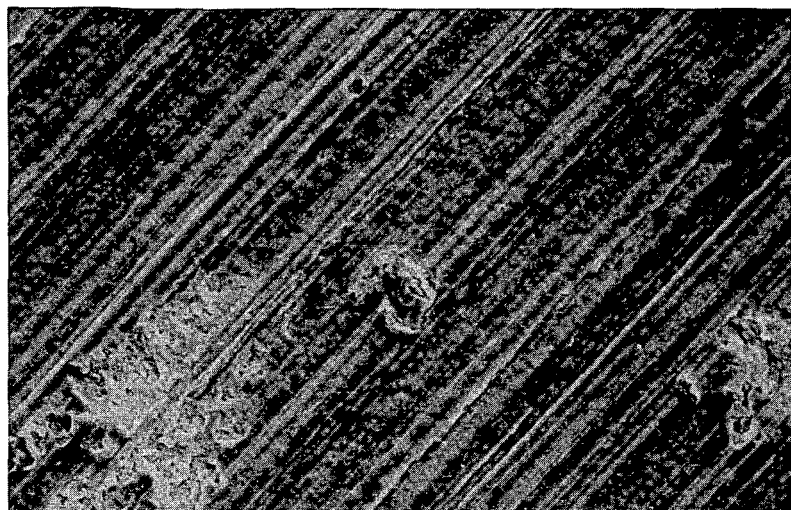
(b)
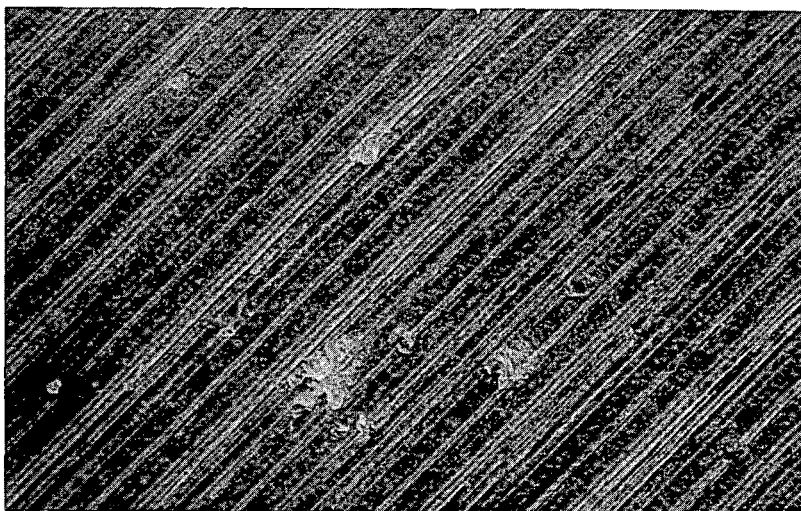
(c)

Fig. 34. Pitting and oxide growth patterns of boron coolant-machined part 5727 shown 225 d after final machining on the OC at 45°. Magnification: (a) 3000X, (b) 1000X, (c) 300X.
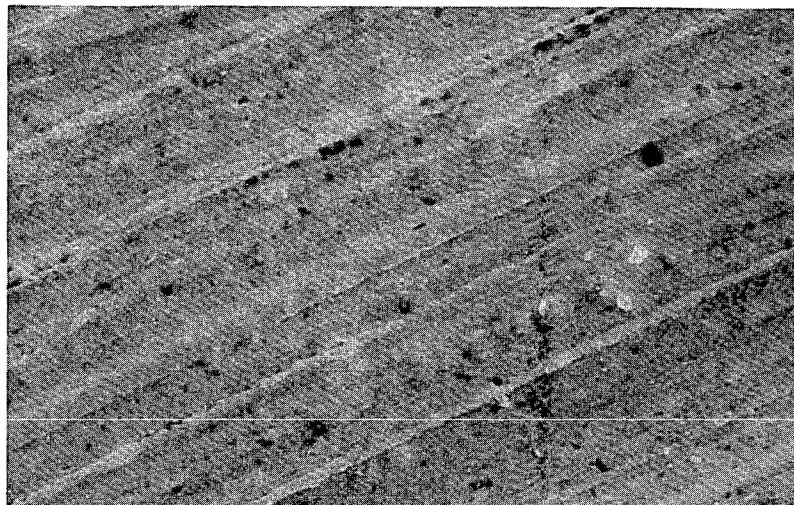
(a)
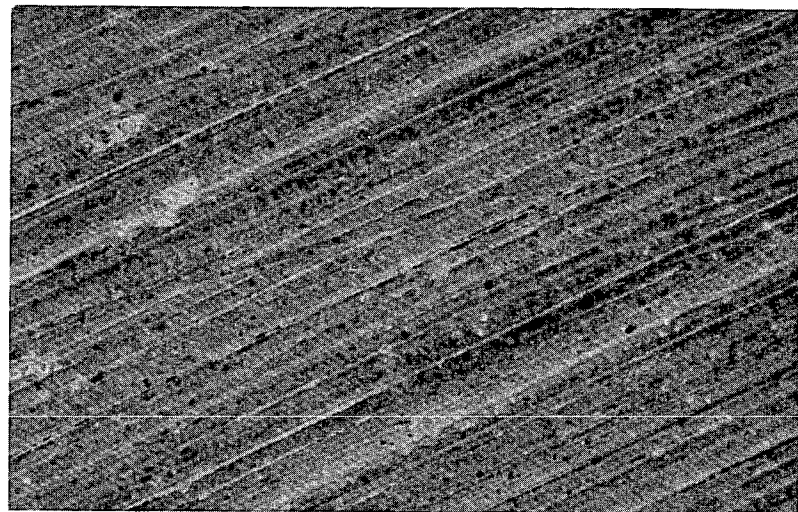
(b)
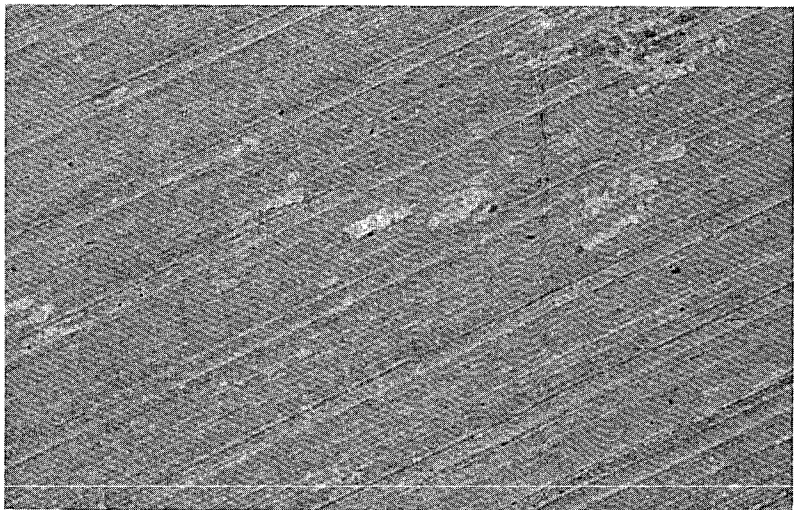
(c)

Fig. 35. Pitting and oxide growth patterns
of perc coolant-machined part 5725 shown 45 d
after final machining on the IC at the mouth.
Magnification: (a) 3000X, (b) 1000X, (c) 300X.

(a)
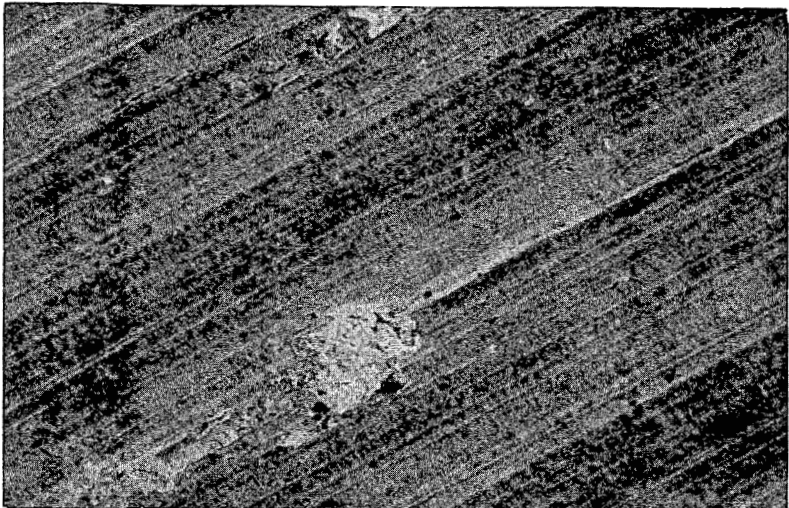
(b)
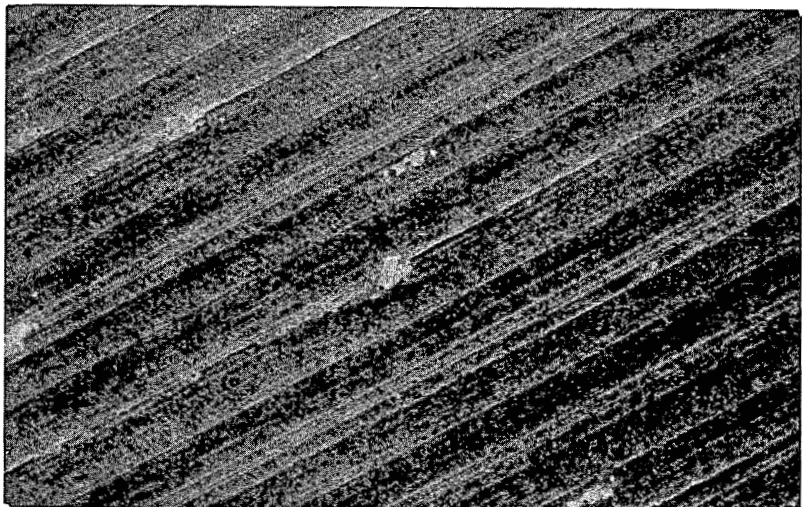
(c)

Fig. 36. Pitting and oxide growth patterns of perc coolant-machined part 5726 shown 45 d after final machining on the IC at the mouth. Magnification: (a) 3000X, (b) 1000X, (c) 300X.

(a)
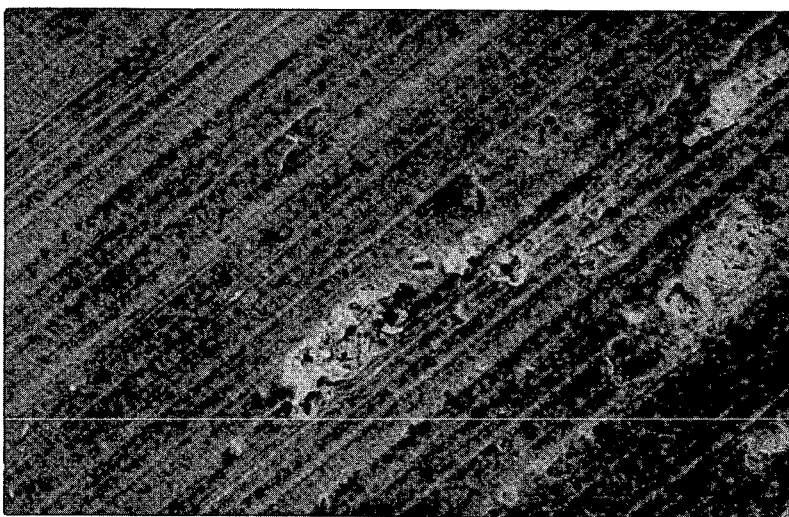
(b)
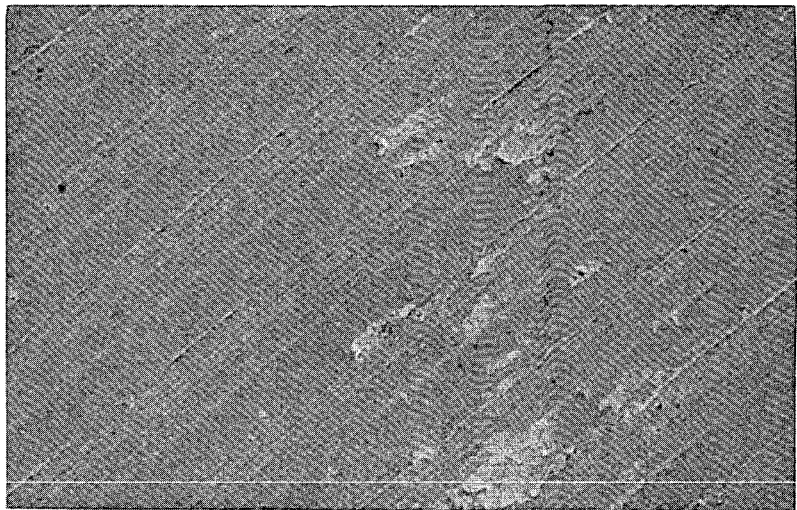
(c)

Fig. 37. Pitting and oxide growth patterns of perc coolant-machined part 5730 shown 75 d after final machining on the IC at the pole. Magnification: (a) 3000X, (b) 1000X, (c) 300X.
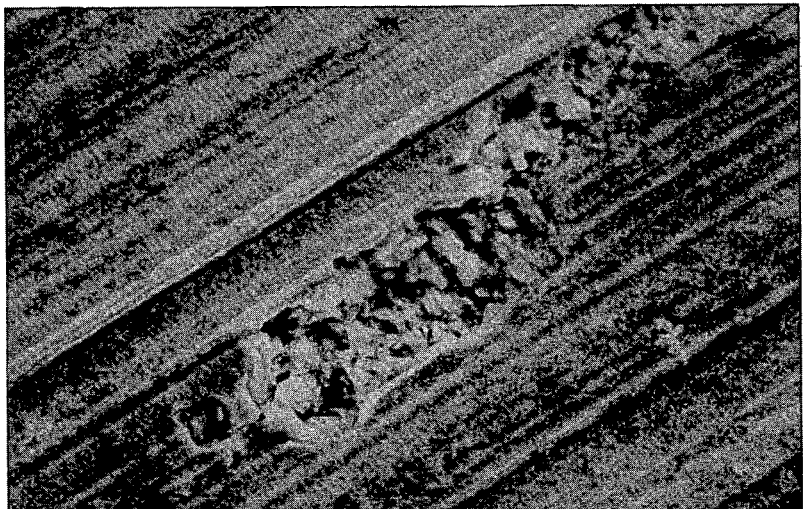
(a)
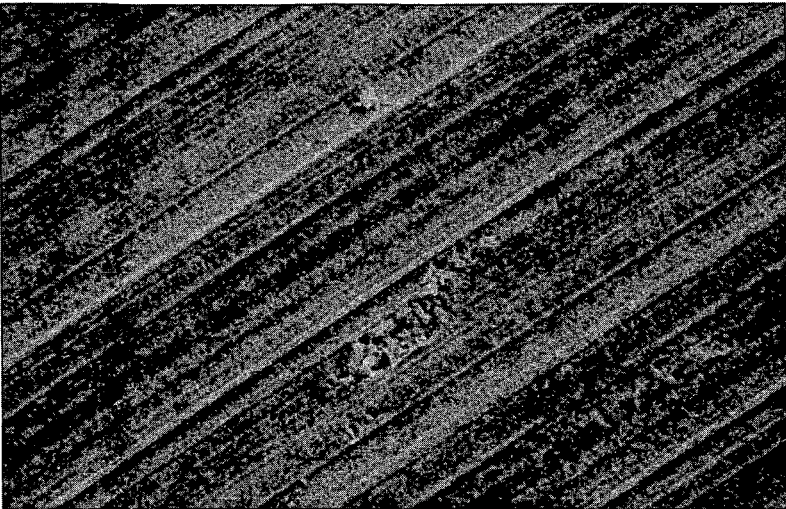
(b)
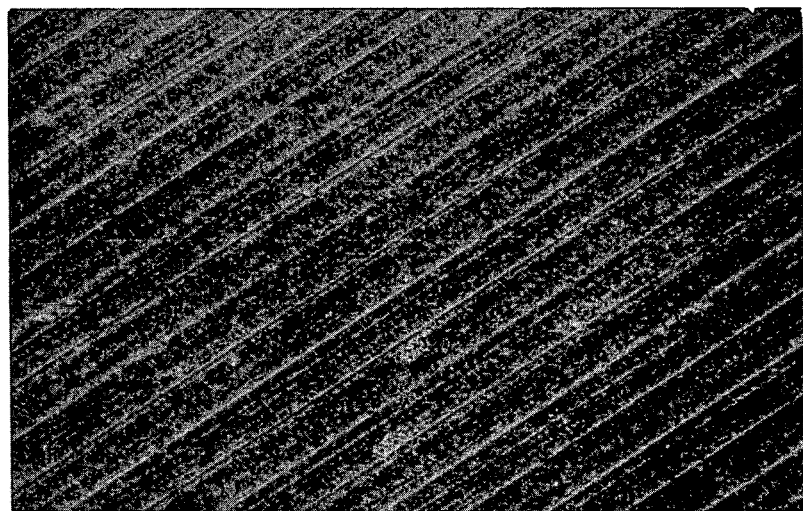
(c)

Fig. 38. Pitting and oxide growth patterns of perc coolant-machined part 5733 shown 75 d after final machining on the OC at the pole. Magnification: (a) 3000X, (b) 1000X, (c) 300X.
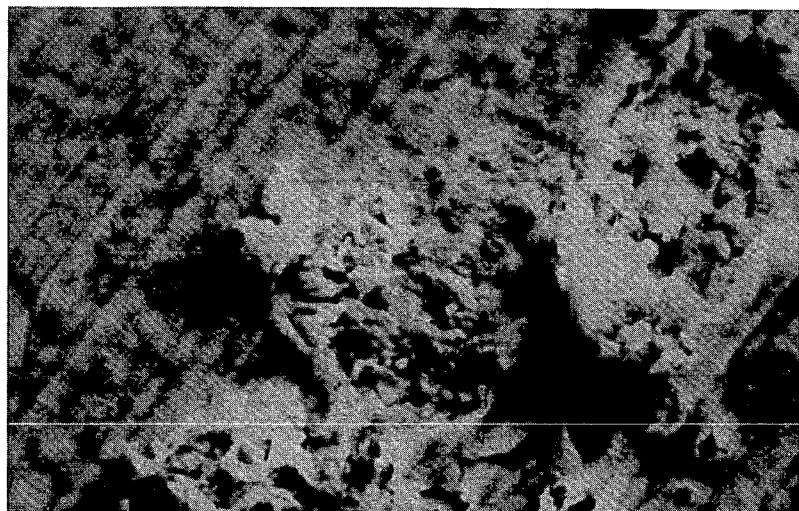
(a)
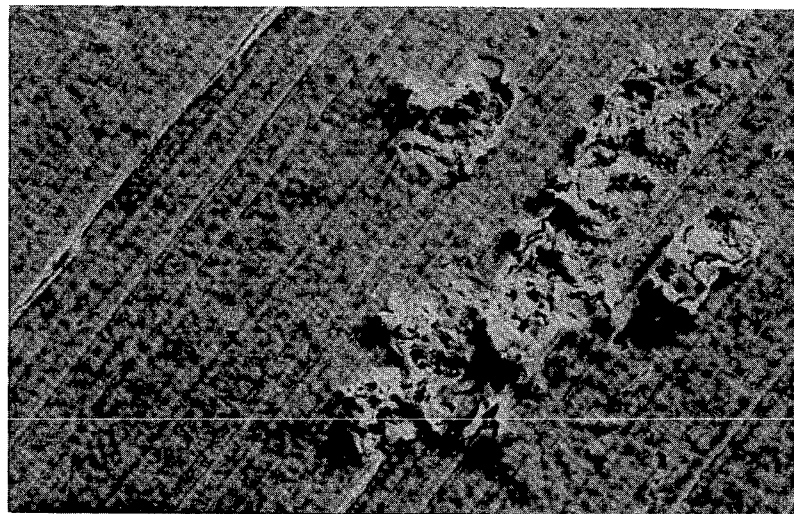
(b)
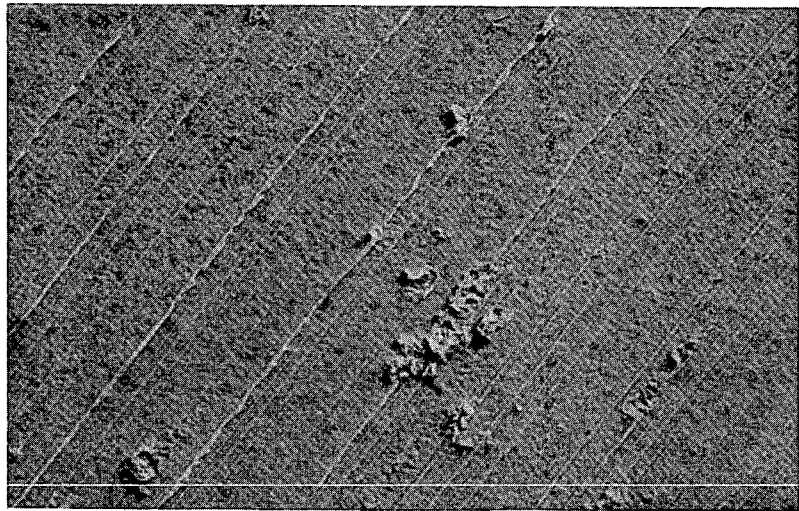
(c)

Fig. 39. Pitting and oxide growth patterns of perc coolant-machined part 5739 shown 225 d after final machining on the IC at 45°. Magnification: (a) 3000X, (b) 1000X, (c) 300X.
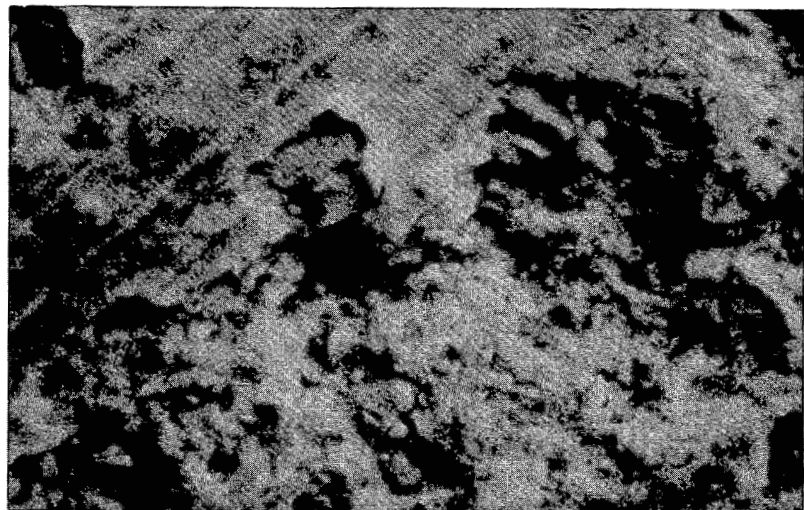
(a)
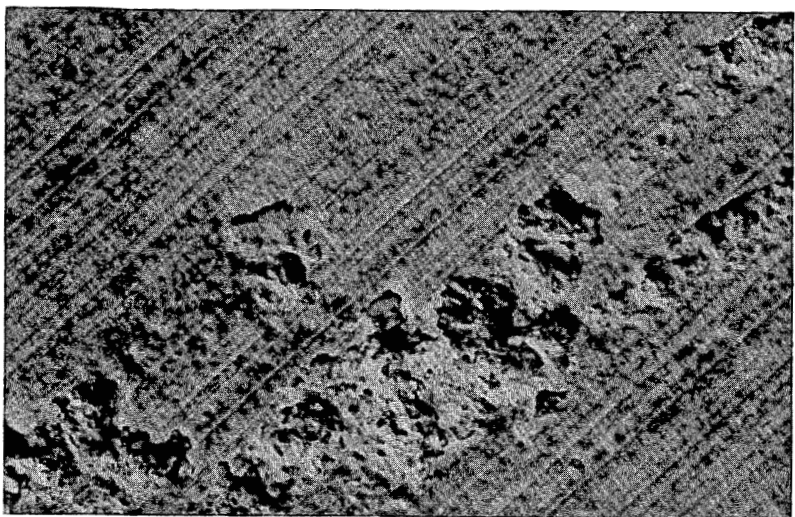
(b)
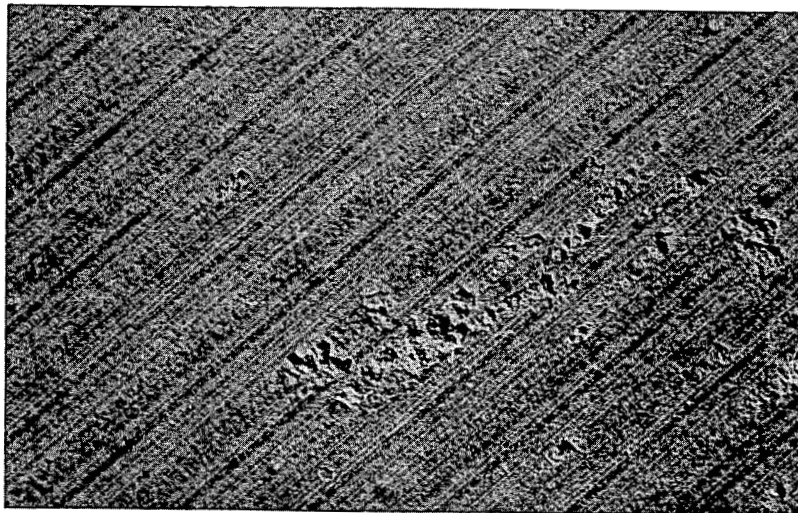

(c)

Fig. 40. Pitting and oxide growth patterns of perc coolant-machined part 5740 shown 225 d after final machining on the OC at 45° Magnification: (a) 3000X, (b) 1000X, (c) 300X.
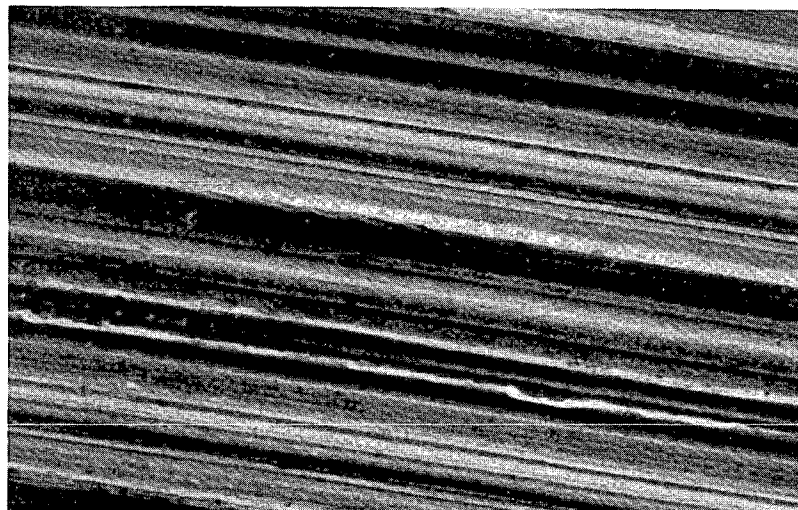
(a)
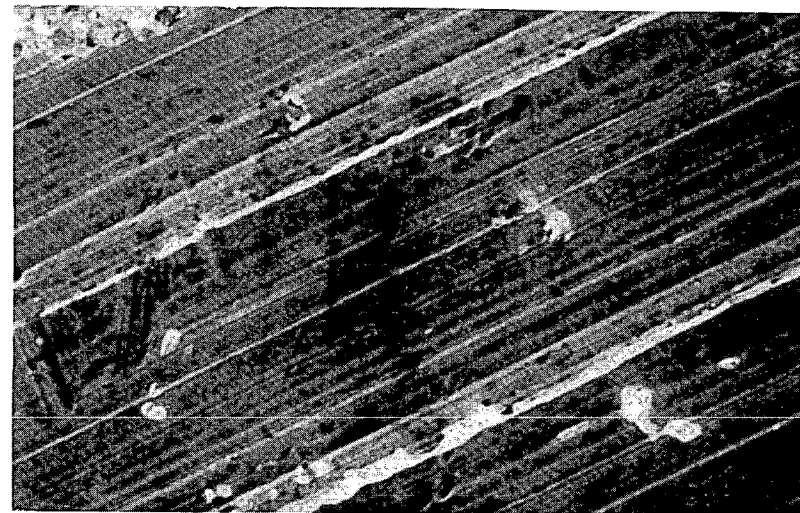
(b)

(c)

(d)

Fig. 41. Surface morphology vs time after final machining—boron coolant. All magnifications are 1000X. Taken after (a) 30 d, (b) 45 d, (c) 75 d, (d) 225 d.
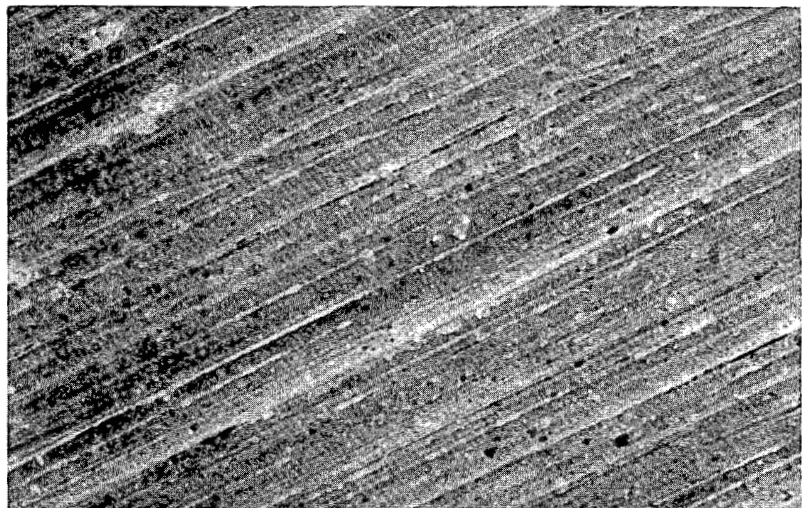
(a)
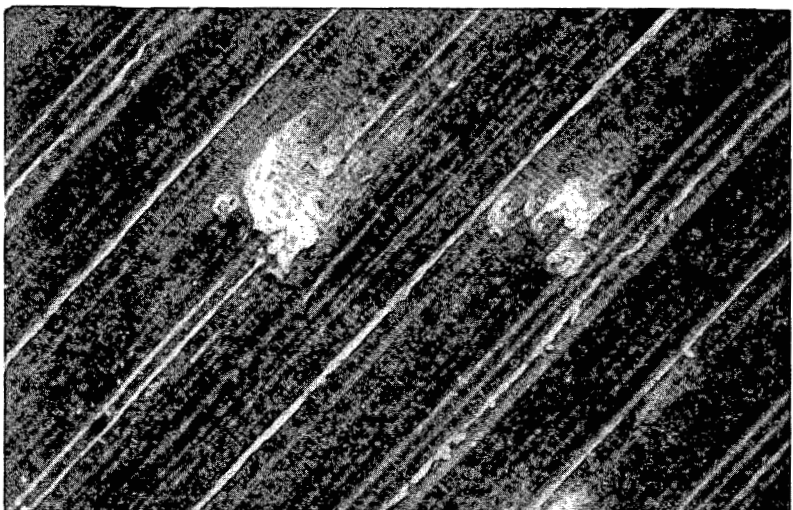
(b)
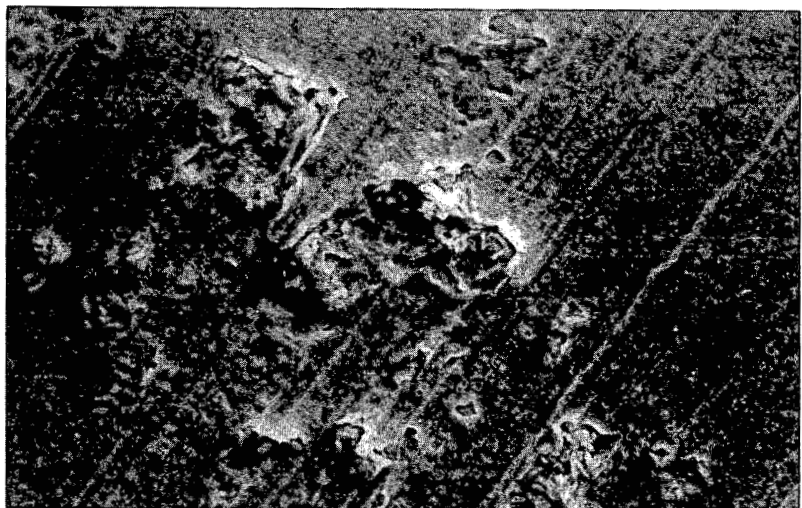
(c)

Fig. 42. Surface morphology vs time after final machining--perchloroethylene coolant. All magnifications are 1000X. Taken after (a) 45 d, (b) 75 d, (c) 225 d.

ACCELERATED CORROSION TESTING

Accelerated corrosion testing was used to determine if there were gross differences in the atmospheric corrosion properties of the enriched uranium machined by the different coolants. The accelerated atmospheric corrosion test consisted of exposing the samples to an alternating humidity cycle at 66°C for approximately 1 month. The humidity cycle was 55 min at 100% relative humidity, 55 min at 50% relative humidity, and a 5-min interval between humidity changes. This alternating condensing/drying cycle causes higher corrosion rates than exposure at a constant humidity.

Prior to exposure, the samples were cleaned with acetone, rinsed with alcohol, and air dried. Each sample was weighed independently by different technicians to the nearest 0.01 mg.

Because of the varying curvature of the samples, the exposed surface area was calculated from thickness, weight, and density rather than from direct dimensional measurement. Also, the edges of most of the specimens contained burrs. If the as-received surface had not been the major concern in the experiment, these burrs would have been removed. Because the purpose of this experiment was to compare coolants and because all samples were handled in the same manner, these perturbations should not have affected the overall results.

After exposure, the samples were washed with alcohol and weighed. A large percentage of the samples had a weight loss, which was attributed to oxide spalling. These weight losses precluded calculating corrosion rates from weight-gain data; therefore, weight-loss data were used. This method of calculating the corrosion rates biases the calculated rates toward the high side because all corrosion is assumed to occur during the 30-d exposure to the alternating humidity environment; in reality, some oxide formed during the storage period.

The basic procedures of ASTM G1-81, "Preparing, Cleaning, and Evaluating Corrosion Test Specimens,"[3] were used to determine corrosion rates. The cleaning solution was 50 vol % nitric acid—50% deionized water at room temperature. Immersion time was 3 min, and the cycle was repeated five times. The first cleaning cycle removed the oxide without significant loss of base metal, and correction factors were not required for base metal removal.

The calculated corrosion rates for the various test conditions are presented in Table 8. The average corrosion rate of the samples that were similar to those sent to Rocky Flats and machined in the propylene glycol-water-borax coolant was 0.45 mil/year. This rate is similar to that of the samples that were machined in this coolant and stored for 1 month: 0.58 and 0.49 mil/year. The corrosion rates of samples machined from the enriched uranium parts that had the standard treatment and those which were stored for an additional month in the Rocky Flats bags were analyzed statistically using a two-factorial design. The main effects were coolant (perc—mineral oil or propylene glycol-water-borax)

and treatment history (standard or standard plus 1 month in Rocky Flats bags). Specimen location within a part was used as a blocking factor. At a 95% confidence level, only the choice of coolant had a significant effect.

Table 8. Corrosion rates of enriched uranium in alternating humidity environment

| Condition | Coolant | Corrosion rate (mil/year) | | | |
		Mouth	45°	Pole	Average
Like Rocky Flats test parts (5715)	Boron	0.37	0.44	0.53	0.45
Standard (5692, 5713)	Boron	0.64	0.66	0.39	0.58
		0.59	0.60	0.57	
Standard (5725, 5726)	Perc	0.77	0.73	0.90	0.83
		0.77	0.96	0.82	
Standard + 1 month in Rocky Flats bags (5720, 5722)	Boron	0.39	0.71	0.56	0.49
		0.50	0.40	0.38	
Standard + 1 month in Rocky Flats bags (5730, 5733)	Perc	1.00[a]	0.45	0.53	0.66
		0.60	0.75	0.62	

[a]Severe localized corrosion.

Additional statistical analysis (see Appendix) indicated that there was a small but significant decrease in the corrosion rate of the 1-month-storage sample compared with the standard treatment samples. This difference may be due to improvements in deburring the samples which were instituted after all the standard treatment samples had been run. This improvement decreased the actual surface area in a way not easily quantifiable.

The corrosion rate of the enriched uranium that was machined with the new propylene glycol-water-borax mixture was 0.23 ± 0.14 mil/year lower than that of the samples machined with the old perc-mineral oil coolant. This slight difference, although insignificant from a practical viewpoint, is in the desired direction and shows that substituting propylene glycol-water-borax coolant for perc-mineral oil coolant will not deleteriously affect the corrosion properties of enriched uranium.

A visual examination of the exposed specimens confirmed the differences in the corrosion characteristics of the specimens machined in the two coolants. Twenty-five percent of the specimens that were machined with the old perc-mineral oil coolant displayed small localized

areas with loose corrosion product (Fig. 43), whereas none of the samples that were machined with the new propylene glycol-water-borax mixture displayed this type of corrosion.

The areas of localized corrosion were evident after a few days' exposure to the test environment and did not appear to grow as the test continued. No efforts were made to determine the cause of these localized corrosion areas; however, they were probably caused by incomplete removal of the chloride contaminant during cleaning operations.

In summary, the corrosion properties of enriched uranium machined in the new propylene glycol-water-borax coolant are superior to those of enriched uranium machined in the old perc-mineral oil coolant. This conclusion is based on both weight-loss data and visual appearance of the exposed specimens.

COOLANT CHARACTERIZATION

To monitor the pickup of contaminants in the coolant and to determine whether the coolant was changing over the course of the machining of our experimental parts, some analyses were run on two 50-mL samples of the boron coolant after machining the first, fourth, seventh, and the tenth parts. These analyses included grams of uranium per gram (gU/g), pH, boron by ICP, propylene glycol-to-water ratio, and ion chromatography for nitrite, nitrate, chloride, and sulfate. The perchloroethylene coolant was collected after the first, third, and fifth parts were machined and the gU/g was determined. The data are displayed in Table 9.

Table 9. Coolant data

| Part | Coolant | Parts per million | | | | | | pH | Glycol/water |
		gU/g	Boron	Cl	NO_2	NO_3	SO_4		
5700	Boron	36.3	8600	32	700	46	26	7.7	41/59
5692	Boron	27.3	8800	28	1000	34	24	7.8	39/61
5727	Boron	28.5	8600	28	740	33	23	7.8	43/57
5715	Boron	29.4	8200	27	710	27	22	7.8	41/59
5740	Perc	38.1							
5739	Perc	37.8							
5733	Perc	38.7							

Note: Machining order--5700, 1st; 5692, 4th; 5727, 7th; and 5715, 10th.
5740, 1st; 5739, 3rd; and 5733, 5th.
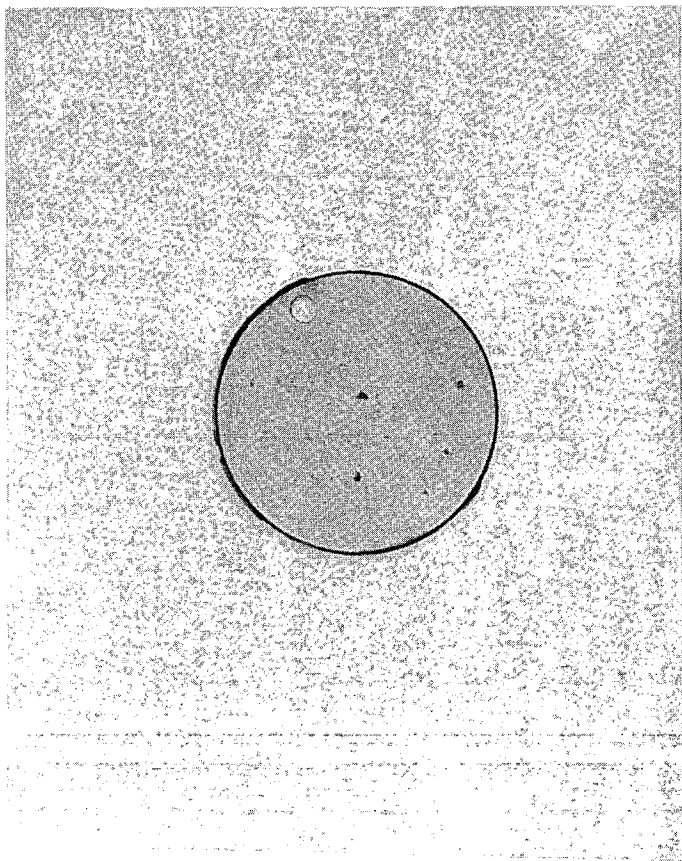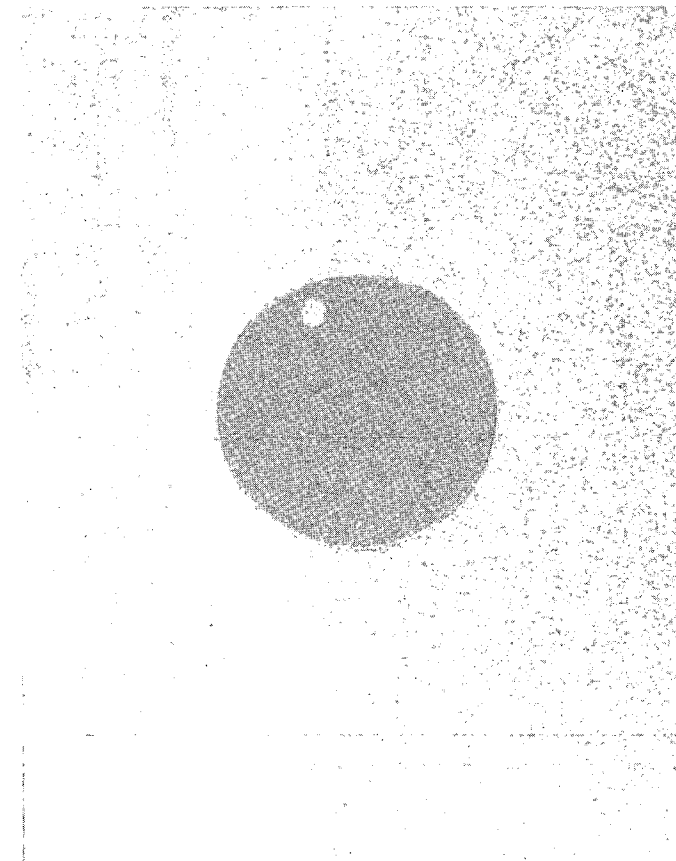
(a)   (b)

Fig. 43.   Samples machined with perc coolant displayed more localized corrosion than did samples machined with the boron coolant.   (a) Perc, 30-d exposure; (b) boron, 30-d exposure.

The only consistent trends in the Table 9 data are decreases in the chloride, nitrate, and sulfate ions with time. The increase in nitrite after the fourth part seems odd. However, the nominal level is 1000 ppm of nitrite as an inhibitor. A favorable note is that the quantity of uranium in the boron coolant did not appear to increase with time and was less than that measured in the perc coolant. The boron level in the coolant is very important, and it appeared to remain stable over the short period of ten parts machined for this study.

A Freon extraction was performed on the coolant associated with parts 5715 and 5727. The former produced 4 mg of residues for 110 mL of coolant. Infrared (IR) analysis showed mineral oil plus unidentified material. The latter produced 48 mg of residues for 114 mL of coolant. An IR analysis indicated that mineral oil was the major component. This amount of mineral oil could easily be some pickup from the perc coolant that had been used in the machine previously.

CONCLUSIONS

Boron residues on the final-finished, boron coolant-machined parts were found to average 15 ± 3 ng/cm^2. Inside contour surfaces averaged somewhat higher than outside contour surfaces. Overall, this level of boron is not considered a problem for any subsequent processing of the parts. General contamination on both perc-machined and boron coolant-machined parts was found to be very similar. Some differences observed were greater boron and carbon on the boron-coolant parts and greater chlorine on the perc-coolant parts. Uranium on the surface of all parts was in the +4 oxidation state. Total oxygen on the surface increased equally for both types of parts with storage time.

After 225 d of exposure, statistically different corrosion rates were found for enriched uranium surfaces machined by the two different coolants and exposed to the normal environmental conditions of the Y-12 Plant. Oxide growth on parts machined with the perc coolant progressed at a rate of 1.6 nm/d vs 1.0 nm/d for the boron coolant-machined parts. Under accelerated corrosion conditions, a slightly higher corrosion rate was found for the perc-cut parts—0.75 mil/year (52 nm/d) vs 0.51 mil/year (35 nm/d) for the boron coolant-cut parts.

During the relatively short term of ten parts machined in the boron coolant, no serious contamination problems of the coolant were discovered, and the boron level remained reasonably constant.

In summary, corrosion resistance of enriched uranium machined with the aqueous propylene glycol–borax coolant is better than that of enriched uranium machined with the perc-mineral oil coolant. The boron residues on the final-finished parts machined using the borax-containing coolant are not sufficient to cause problems in further processing. All evidence indicates that the enriched uranium surfaces machined using the borax-containing coolant will be as satisfactory as those machined using the perc coolant.

ACKNOWLEDGMENTS

REFERENCES

1. G. C. Allen and P. M. Tucker, *J. Chem. Soc. Dalton Trans.* 470, (1973).

2. J. A. Happe, C. A. Colmenares, T. McCreary, and G. A. Somorjai, SUBWOG 12 Meeting at GEND, St. Petersburg, Fla., Feb. 16-18, 1977.

3. *Annual Book of ASTM Standards*, vol. 10, American Society for Testing and Materials, Philadelphia, 1981.

APPENDIX

STATISTICAL ANALYSIS OF DATA

A.1 SURFACE CONTAMINATION

A.1.1 Boron Results

Because of the variability and inconsistency in the bulk boron data, the approach to assessing surface boron by subtracting the average bulk boron from the boron levels found in the chips appears to be unreliable. As the report suggests, acid leaching is probably the most reliable approach for assessing surface boron. Six-cm-diam disks were cut from each of n = 6 parts machined with the boron coolant and from each of n = 5 parts machined with the perchloroethylene (perc) coolant. The disks were acid leached to remove surface boron, and the leachant was measured for boron content by inductively coupled plasma emission spectroscopy (ICP). The acid leaching results are as follows:

Coolant	Part	Surface boron (ng/cm^2)
Boron	5715	12
Boron	5692	19
Boron	5713	16
Boron	5720	16
Boron	5722	13
Boron	5727	16
Perc	5726	a
Perc	5730	a
Perc	5733	a
Perc	5739	a
Perc	5740	a

aBelow ICP detection limit.

Since the surface boron results for the perc coolant are all below the detection limit of the ICP spectroscopy, it is not possible to statistically compare the levels of surface boron for the two coolants. It is possible, however, to estimate the mean surface boron level for the boron coolant. A 95% confidence interval for this mean surface boron level is 15.3 ± 2.6 ng/cm^2.

A.1.2 ESCA Results

Electron spectroscopy (ESCA) was used to assess the surface conditions of the machined parts in terms of three atomic concentration ratios: O(1s)HBE/O(1s)LBE, O(1s)/U(4f), and C(1s)/U(4f). These three ratios were determined at each of three positions (pole, 45°, and mouth)

on each of twelve parts. An analysis of variance was performed to statistically compare the means of seven handling treatments, as well as to compare the means at the three positions (pole, 45°, and mouth) and to assess any possible interaction between treatment and position. The treatment means and the analysis of variance results are given in Tables A.1 and A.2 respectively.

Taking as statistically significant any F-test for which the p-value (probability >F) falls below p = 0.05, we can conclude the following:

1. For both coolants, the means of each of the three ratios O/O, O/U, and C/U increase significantly with storage time. This increase can be modeled by straight lines for all three ratios. For the O/U and C/U ratios, no matter which coolant is considered, the least-squares regression lines are

    O/U = 2.734 + 0.016 (storage time, d),

    C/U = 2.972 + 0.044 (storage time, d).

    For the O/O ratio, statistical evidence suggests that the two coolants have different regression lines:

    Boron coolant:

    O/O ≡ 0.944 + 0.012 (storage time, d),

    Perc coolant:

    O/O = 0.027 (storage time, d).

    Thus the two coolants behave similarly with respect to either their O/U or C/U ratios as a function of storage time. However, for the O/O ratio, the least-squares regression lines indicate that the O/O ratio is lower for the perc coolant than for the boron coolant for less than 64 d of storage, but the O/O ratio is greater for the perc coolant than for the boron coolant for more than 64 d of storage.

2. The means of each of three ratios do not differ significantly among the three sampling positions (pole, 45°, and mouth).

3. There is no evidence of any interaction between position and treatment for any of the three ratios.

See Figs. A.1, A.2, and A.3 for plots of the O/O, O/U, and C/U treatment means.

Table A.1. ESCA sample means

Treatment	Coolant	Handling	Storage time (d)	n	Means		
					O/O	O/U	C/U
1	Boron	Same as Rocky Flats Plant	30	3	1.34	3.08	5.42
2	Boron	Standard	45	6	1.40	3.60	5.45
3	Perc	Standard	45	6	1.44	3.43	4.32
4	Boron	Standard + 1 month	75	6	1.94	4.10	6.88
5	Perc	Standard + 1 month	75	6	1.62	3.70	5.23
6	Boron	Standard + 6 months	225	3	3.64	6.05	10.97
7	Perc	Standard + 6 months	225	6	6.10	6.47	14.11

A.2 OXIDE DEPTH RESULTS

The ion microprobe mass analyzer (IMMA) was used to measure the depth of the oxide corrosion layer on coupons cut from each of six locations [three positions (pole, 45°, and mouth) on two surfaces (IC and OC)] on each of twelve parts. An analysis of variance was performed to look for effects on the mean oxide depth due to the different handling treatments, the three positions, or the two surfaces, and to look for any interactions among the three factors. The analysis of variance results and the appropriate sample means are given in Tables A.3 and A.4, respectively.

The mean oxide depth increases significantly with storage time on both the parts machined with the boron coolant and the parts machined with the perc coolant. This increase in oxide depth can be modeled as a straight-line function of storage time, but the equation of the line depends on the coolant type and on the measurement position (IC or OC; pole, 45°, or mouth) (see Fig. A.4).

Even though the equations for the lines depicting the relationship between oxide depth and storage time do change with coolant and measurement position, a reasonable way to approximate the overall relationship between the oxide depth on the parts and storage time is to fit one regression line using all the data for the perc-machined parts and

Table A.2. ESCA analysis of variance

Source	D.F.	Probability >F[a]		
		0/0	0/U	C/U
Treatment[b]	6			
a. Storage time		0.0014	0.0003	0.0055
Linear		0.0005	0.0001	0.0020
Quadratic		0.5968	0.7345	0.9287
b. Coolant		0.1005	0.8109	0.9177
c. Storage time X coolant		0.0619	0.3423	0.2629
Linear X coolant		0.0275	0.2019	0.1283
Quadratic X coolant		0.3659	0.4673	0.6082
d. Linear storage time (boron coolant)		0.0215	0.0008	0.0420
e. Quadratic storage time (boron coolant)		0.9147	0.3817	0.9183
f. Cubic storage time (boron coolant)		0.8063	0.6364	0.7892
Part (treatment)	5			
Position	2	0.8585	0.2509	0.2664
Position X treatment	12	0.8131	0.0914	0.1864
Residual	10			
Total	35			

[a]An analysis of variance was also performed on the rank transformed data, because the response variables are ratios that do not follow a normal distribution. Results for the analysis of variance on the original data and on the rank transformed data were similar (taking $\alpha = 0.05$).

[b]Contrasts a, b, and c involve treatments 2 through 7 only. Contrasts d, e, and f involve treatments 1, 2, 4, and 6.

Y-GA 86-944

OXYGEN RATIO

7
6
5
4
3
2
1

PERC COOLANT

BORON COOLANT

0 20 40 60 80 100 120 140 160 180 200 220 240
STORAGE TIME (DAYS)
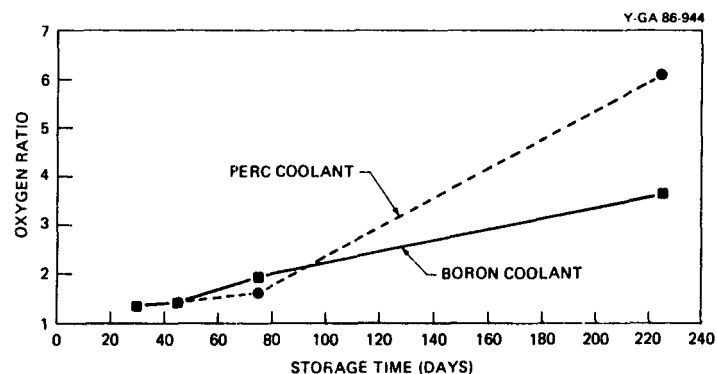
Fig. A.1. Plot of O(1s)HBE/O(19)LBE treatment means versus days of storage.

Y-GA 86-945

O TO U RATIO

7
6
5
4
3
2

PERC COOLANT

BORON COOLANT

0 20 40 60 80 100 120 140 160 180 200 220 240
STORAGE TIME (DAYS)
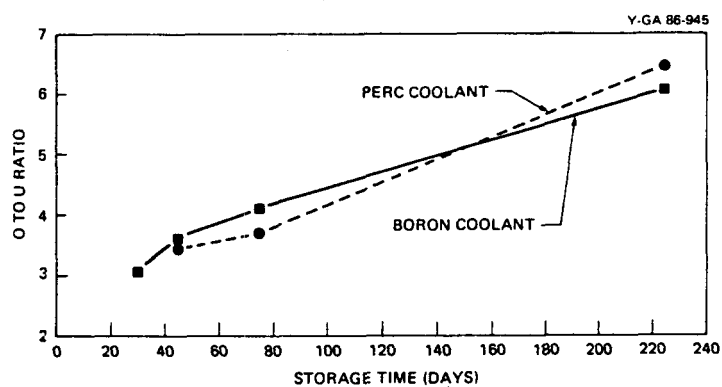
Fig. A.2. Plot of O(1s)/U(4f) treatment means versus days of storage.

Y-GA 86-946

C TO U RATIO

15.0
12.5
10.0
7.5
5.0
2.5
0

BORON COOLANT

PERC COOLANT

20 40 60 80 100 120 140 160 180 200 220 240
STORAGE TIME (DAYS)
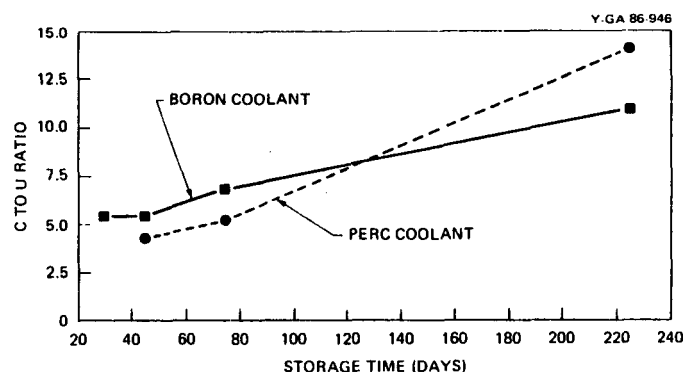
Fig. A.3. Plot of C(1s)/U(4f) treatment means versus days of storage.

Table A.3. Oxide depth analysis of variance

Source	D.F.	Probability >F
Treatment	6	
a. Storage time		0.0001
Linear		0.0001
Quadratic		0.1078
b. Coolant		0.0023
c. Storage time X coolant		0.0043
Linear X coolant		0.0017
Quadratic X coolant		0.1940
Part (treatment)	5	
Position	2	0.0017
Surface	1	0.0025
Position X surface	2	0.0020
Treatment X position	12	0.0023
Treatment X surface	6	0.0001
Treatment X position X surface	12	0.0090
Residual	25	
Total	71	

Note: Contrasts a, b, and c involve treatments 2 through 7 only.

separately fit a second regression line using all the data for the boron-machined parts (i.e., combine data from all six measurement positions) (see Fig. A.5). The least-squares regression lines fitted using these combined data are:

Boron coolant:

Oxide depth (nm) = 62.983 + 0.983 (storage time, d),

Perc coolant:

Oxide depth (nm) = 42.398 + 1.638 (storage time, d).

Table A.4. Oxide depth sample means

Treatment	Coolant	Handling	Storage time (d)	n	Mean oxide depth (nm)
1	Boron	Same as Rocky	30	6	63.9
2	Boron	Standard	45	12	101.0
3	Perc	Standard	45	12	114.0
4	Boron	Standard + 1 month	75	12	162.7
5	Perc	Standard + 1 month	75	12	167.8
6	Boron	Standard + 6 months	225	6	273.1
7	Perc	Standard + 6 months	225	12	410.6

| Treatment	Coolant	Position	Surface	Storage time (d)	Mean oxide depth (nm)
1	Boron	Mouth	IC	30	109.0
2	Boron	Mouth	IC	45	84.0
4	Boron	Mouth	IC	75	128.5
6	Boron	Mouth	IC	225	164.5
1	Boron	Mouth	OC	30	82.5
2	Boron	Mouth	OC	45	133.0
4	Boron	Mouth	OC	75	204.7
6	Boron	Mouth	OC	225	401.0
1	Boron	Pole	IC	30	36.5
2	Boron	Pole	IC	45	89.0
4	Boron	Pole	IC	75	175.0
6	Boron	Pole	IC	225	149.0
1	Boron	Pole	OC	30	53.0
2	Boron	Pole	OC	45	100.0
4	Boron	Pole	OC	75	195.0
6	Boron	Pole	OC	225	260.3
1	Boron	45°	IC	30	61.5
2	Boron	45°	IC	45	81.8
4	Boron	45°	IC	75	143.8
6	Boron	45°	IC	225	336.7
1	Boron	45°	OC	30	41.0
2	Boron	45°	OC	45	114.7
4	Boron	45°	OC	75	131.0
6	Boron	45°	OC	225	327.0
3	Perc	Mouth	IC	45	117.5
5	Perc	Mouth	IC	75	196.0
7	Perc	Mouth	IC	225	408.7
3	Perc	Mouth	OC	45	127.7
5	Perc	Mouth	OC	75	184.0
7	Perc	Mouth	OC	225	418.3
3	Perc	Pole	IC	45	89.3
5	Perc	Pole	IC	75	148.5
7	Perc	Pole	IC	225	446.5
3	Perc	Pole	OC	45	114.5
5	Perc	Pole	OC	75	153.8
7	Perc	Pole	OC	225	361.8
3	Perc	45°	IC	45	108.8
5	Perc	45°	IC	75	172.0
7	Perc	45°	IC	225	436.7
3	Perc	45°	OC	45	126.8
5	Perc	45°	OC	75	154.8
7	Perc	45°	OC	225	391.5

64
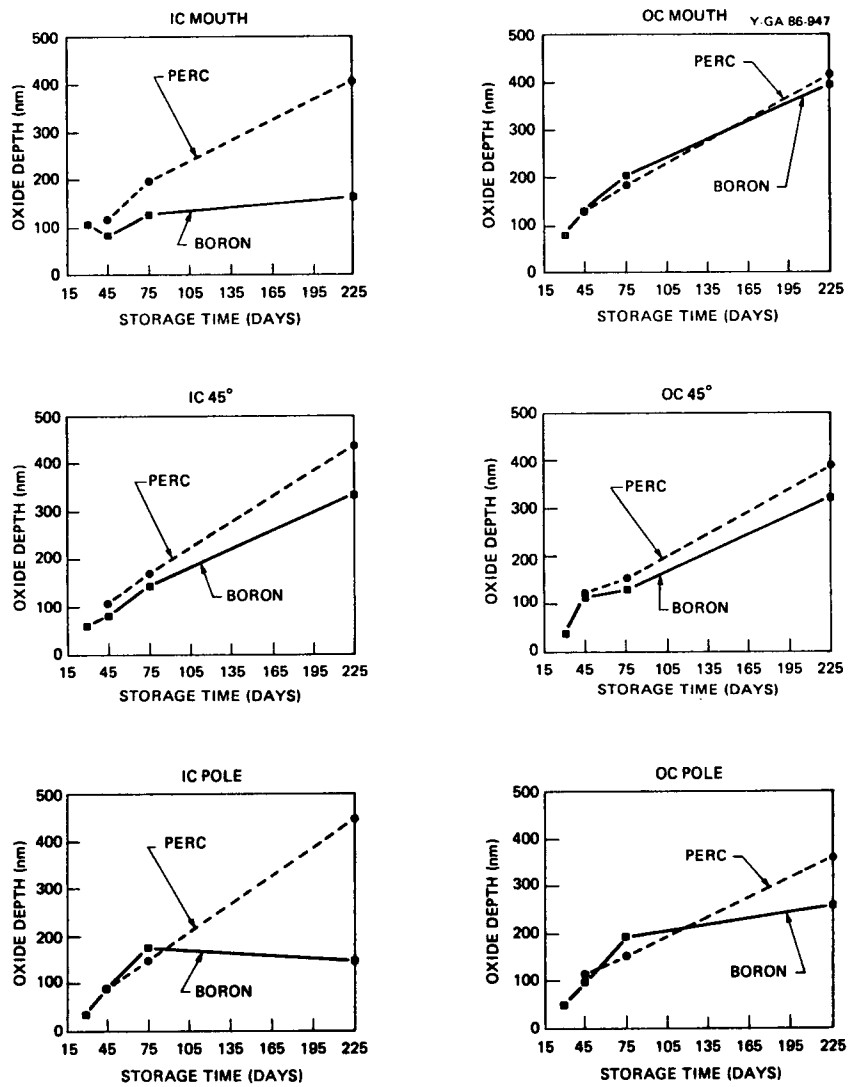
**Fig. A.4. Plot of oxide depth treatment means versus days of storage (by surface and position).**
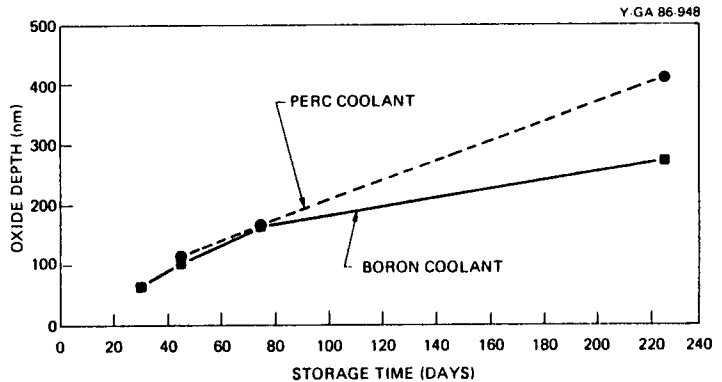
Fig. A.5. Plot of oxide depth treatment means versus days of storage.

These two regression equations indicate that for 30 to 31 d of storage, the boron-machined parts have greater oxide depth than the perc-machined parts; for 31-225 d of storage, the boron-machined parts have lower oxide depth than the perc-machined parts.

A.3 SURFACE MORPHOLOGY AND LOCAL CORROSION

No data are available.

A.4 ACCELERATED CORROSION TEST RESULTS

Samples from nine parts were subjected to an accelerated corrosion test. The corrosion rate (mils per year) was determined for a sample from each of three positions (pole, $45°$, and mouth) on each of nine parts. An analysis of variance was performed to look for effects on the mean corrosion rate due to the different handling treatments or due to the three positions, and to look for an interaction between position and treatment. The analysis of variance results and sample means are given in Tables A.5 and A.6, respectively.

Table A.5. Accelerated corrosion analysis of variance

Source	D.F.	Probability >F
Treatment	4	
Storage time		0.0219
Coolant		0.0038
Storage time X coolant		0.3027
Linear storage time (boron coolant)		0.7540
Quadratic storage time (boron coolant)		0.0802
Part (treatment)	4	
Position	2	0.9301
Position X treatment	8	0.8153
Residual	8	
Total	26	

Table A.6. Accelerated corrosion sample means

Treatment	Coolant	Handling	Storage time (d)	n	Mean corrosion rate (mil/year)
1	Boron	Same as Rocky	30	3	0.45
2	Boron	Standard	45	6	0.58
3	Perc	Standard	45	6	0.83
4	Boron	Standard + 1 month	75	6	0.49
5	Perc	Standard + 1 month	75	6	0.66

From the analysis of variance results, we can conclude the following:

1. There is a significant decrease in the mean corrosion rate from 45 to 75 d of storage for both the boron and perc coolants.

2. The perc coolant mean corrosion rate is significantly higher than the boron coolant mean corrosion rate.

3. There is no significant interaction between storage time and coolant.

4. There is no significant difference in the mean corrosion rate for the three positions (pole, 45°, and mouth).

5. There is no significant interaction between position and treatment.

See Fig. A.6 for a plot of the corrosion rate treatment means.

A.5 COOLANT CHARACTERIZATION

As part machining progressed, contaminants in the coolant were monitored. Only the uranium content was monitored both in the boron and perc coolants. There are not enough data to reliably assess the existence of any trend in uranium levels in the coolants as a function of the number of parts machined. The data that were collected on uranium content of the two coolants are displayed in Fig. A.7.
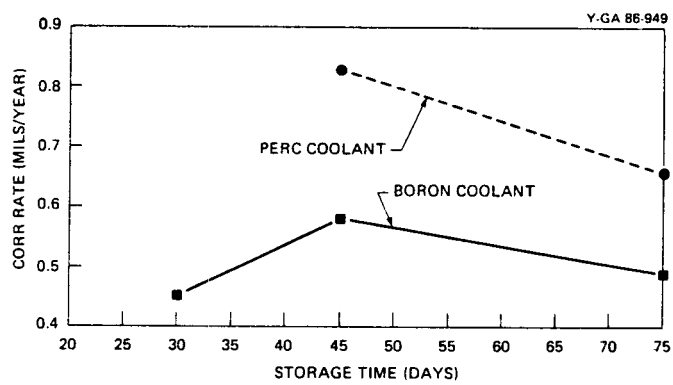
Fig. A.6. Plot of corrosion rate
treatment means versus days of storage.
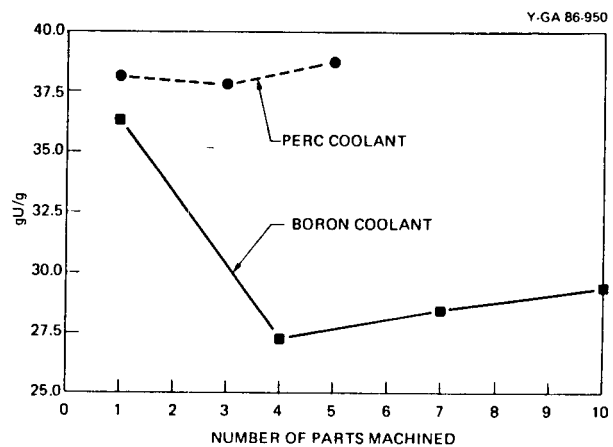
Fig. A.7. Plot of uranium
concentration in coolant versus
number of parts machined.

Distribution

Department of Energy - Oak Ridge

Poteat, R. M.
Spence, R. J.

Lawrence Livermore National Laboratory

Clough, R. E./Galles, H. L.
Miller, G. H.
Ragaini, R. C.
Robbins, J. L.
Sanford, C. B.
Seaton, D. L.
Shuler, W. B./Wraith, C. L.
Technical Information Division
Werne, R. W./Grissom, M. L.

Los Alamos National Laboratory

Dunning, D. N.
Hoyt, H. C.
Waugh, H. G.

Oak Ridge Y-12 Plant

Ardary, Z. L.
Arehart, Jr., T. A.
Asbury, W. L.
Barkman, J. R.
Bennett, R. K.
Burditt, R. B.
Bryant, D. P.
Butler, H. R.
Chapman, L. R.
Cochran, J. L.
Creech, E. T.
Cristy, S. S. (5)
Dean, L. A.
Dillon, J. J.
Dodson, W. H./Googin, J. M.
Duerksen, W. K.
Dyer, E. B.
Fee, G. G.
Ferguson, J. E.
Garber, J. W.
Golshani, A. M.
Guinn, G. R.
Johnson, D. H.
Jones, F. W.
Jones, L. P.
Keith, A.

Keyser, R. M.
Kite, H. T.
Koger, J. W.
Kollie, T. G.
Kosinski, F. E./Napier, J. M.
Lambdin, Jr., F.
Larson, G. F.
McAlister, R. J.
Mills, Jr., J. M.
Needham, E. D.
Post, D. W.
Richards, H. L.
Seals, R. D.
Shelton, J. T.
Smith, D. W.
Steger, P. J./Roettger, F. J.
Stephenson, M. J.
Taylor, P. A.
Thompson, Jr., W. H.
Townsend, A. B.
Walton, Y. W.
Williams, R. D.
Yaggi, W. J.
Y-12 Central Files (Master)
Y-12 Central Files (Route)
Y-12 Central Files (Y-12RC)
Y-12 Central Files (5)

Paducah Gaseous Diffusion Plant

Walter, C. W.

Rockwell International-Rocky Flats

Cleavenger, R. D.
Crisler, L. R.
Dorr, J. E.

Sandia National Laboratories - Livermore

Olson, D. M.

In addition, this report is distributed in accordance with the Category UC-25, **Materials**, as given in the Standard Distribution for *Unclassified Scientific and Technical Reports*, DOE/TIC-4500.